Journal Pre-proofs

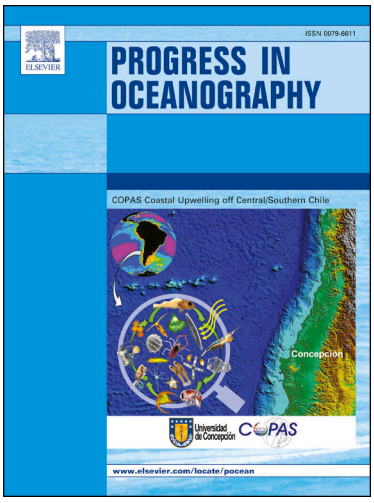

Spatial models cannot compensate for sampling designs unstructured relative to isotopic variation: implications for baseline isoscape development in the Mediterranean Sea

Sarah Magozzi, Clive N. Trueman, Matthew R.D. Cobain, Kirsteen M. MacKenzie, Katie St. John Glew, José A. Canseco, Eric Díaz-Delgado, Emanuela Fanelli, Paola Rumolo, Joan E. Cartes, Boris Espinasse, Davide Agnetta, Marta Albo-Puigserver, Carme Alomar, Francesca Alvisi, Fabio Badalamenti, Daniela Bănaru, Daniela Berto, Angelo Bonanno, Chiara Bonaviri, Lucia Bongiorni, Yeşim Büyükateş, Antonio M. Calafat Frau, Elisa Camatti, Carolina Cantoni, Luis Cardona, Antoine Carlier, Michela Castellano, Spyros Chaikalis, Jacopo Chiggiato, Tamara Cibic, Pascal Conan, Ilaria Conese, Martina Coppari, David Costalago, Pierre Cresson, Isabella D'Ambra, Kirstin Dähnke, Audrey M. Darnaude, Salud Deudero, Daria Ezgeta-Balić, Michele Giani, Alexandra Gogou, Gérald Grégori, Tamar Guy-Haim, Mireille L. Harmelin-Vivien, Simon Jennings, Aristomenis P. Karageorgis, Rolf Koppelmann, Nikolaos Lampadariou, Leonardo Langone, Camilla Liénart, Maria Grazia Mazzocchi, Antonio Mazzola, Travis B. Meador, Louise Merquiol, Marc Metzke, Stefano Miserocchi, Jürgen Möbius, Behzad Mostajir, Laure Mousseau, Joan Navarro, Nives Ogrinc, Marco Pansera, Silvio Pantoja-Gutiérrez, Vanesa Papiol, Constantine Parinos, Catalina Pasqual, Alexandra Pavlidou, Rut Pedrosa-Pàmies, John Pinnegar, Nicholas V.C. Polunin, Maria Protopapa, Daniel J. Repeta, Nadia Sabatino, Julian P. Sachs, Anna Sanchez-Vidal, Gianluca Sarà, Nicolas Savoye, Anna Schroeder, Ester Skylaki, Daniel M. Sigman, Geraldina Signa, Guy Sisma-Ventura, Ioanna Stavrakaki, Ulrich Struck, Javier A. Tesán-Onrubia, Tommaso Tesi, Sinan Uzundumlu, Maria Valls, Salvatrice Vizzini, Soultana Zervoudaki, Salem W. Zgozi, Annamaria Zoppini, Barbara Zorica, Trevor J. Willis

PII: S0079-6611(26)00128-X
DOI: https://doi.org/10.1016/j.pocean.2026.103794
Reference: PROOCE 103794

To appear in: *Progress in Oceanography*

Received Date: 26 November 2025
Revised Date: 19 June 2026
Accepted Date: 2 July 2026

Please cite this article as: Magozzi, S., Trueman, C.N., Cobain, M.R.D., MacKenzie, K.M., John Glew, K.S., Canseco, J.A., Díaz-Delgado, E., Fanelli, E., Rumolo, P., Cartes, J.E., Espinasse, B., Agnetta, D., Albo-Puigserver, M., Alomar, C., Alvisi, F., Badalamenti, F., Bănaru, D., Berto, D., Bonanno, A., Bonaviri, C., Bongiorni, L., Büyükateş, Y., Calafat Frau, A.M., Camatti, E., Cantoni, C., Cardona, L., Carlier, A., Castellano, M., Chaikalis, S., Chiggiato, J., Cibic, T., Conan, P., Conese, I., Coppari, M., Costalago, D., Cresson, P., D'Ambra, I., Dähnke, K., Darnaude, A.M., Deudero, S., Ezgeta-Balić, D., Giani, M., Gogou, A., Grégori, G., Guy-Haim, T., Harmelin-Vivien, M.L., Jennings, S., Karageorgis, A.P., Koppelmann, R., Lampadariou, N., Langone, L., Liénart, C., Mazzocchi, M.G., Mazzola, A., Meador, T.B., Merquiol, L., Metzke, M., Miserocchi, S., Möbius, J., Mostajir, B., Mousseau, L., Navarro, J., Ogrinc, N., Pansera, M., Pantoja-Gutiérrez, S., Papiol, V., Parinos, C., Pasqual, C., Pavlidou, A., Pedrosa-Pàmies, R., Pinnegar, J., Polunin, N.V.C., Protopapa, M., Repeta, D.J., Sabatino, N., Sachs, J.P., Sanchez-Vidal, A., Sarà, G., Savoye, N., Schroeder, A., Skylaki, E., Sigman, D.M., Signa, G., Sisma-Ventura, G., Stavrakaki, I., Struck, U., Tesán-Onrubia, J.A., Tesi, T., Uzundumlu, S., Valls, M., Vizzini, S., Zervoudaki, S., Zgozi, S.W., Zoppini, A., Zorica, B., Willis, T.J., Spatial models cannot compensate for sampling designs unstructured relative to isotopic variation: implications for baseline isoscape development in the Mediterranean Sea, *Progress in Oceanography* (2026), doi: https://doi.org/10.1016/j.pocean.2026.103794

Spatial models cannot compensate for sampling designs unstructured relative to isotopic variation: implications for baseline isoscape development in the Mediterranean Sea

Sarah Magozzi[a,b,c,*], Clive N. Trueman[d], Matthew R. D. Cobain[e], Kirsteen M. MacKenzie[f], Katie St. John Glew[d], José A. Canseco[g], Eric Díaz-Delgado[h,c], Emanuela Fanelli[i,j,b], Paola Rumolo[k], Joan E. Cartes[l], Boris Espinasse[m], Davide Agnetta[n,b], Marta Albo-Puigserver[o], Carme Alomar[o], Francesca Alvisi[p], Fabio Badalamenti[q,b,r], Daniela Bănaru[s], Daniela Berto[t], Angelo Bonanno[u], Chiara Bonaviri[c,v], Lucia Bongiorni[w], Yeşim Büyükateş[x], Antonio M. Calafat Frau[y], Elisa Camatti[w], Carolina Cantoni[z], Luis Cardona[aa], Antoine Carlier[ab], Michela Castellano[a], Spyros Chaikalis[ac,†], Jacopo Chiggiato[w], Tamara Cibic[ad], Pascal Conan[ae,†], Ilaria Conese[p], Martina Coppari[i,b], David Costalago[af], Pierre Cresson[f], Isabella D'Ambra[ag], Kirstin Dähnke[ah], Audrey M. Darnaude[ai], Salud Deudero[o], Daria Ezgeta-Balić[aj], Michele Giani[ak], Alexandra Gogou[ac], Gérald Grégori[s], Tamar Guy-Haim[al], Mireille L. Harmelin-Vivien[s], Simon Jennings[am,an], Aristomenis P. Karageorgis[ac], Rolf Koppelmann[ao], Nikolaos Lampadariou[ap], Leonardo Langone[aq], Camilla Liénart[ar], Maria Grazia Mazzocchi[ag], Antonio Mazzola[v,bh], Travis B. Meador[as,at], Louise Merquiol[s,ag], Marc Metzke[ah,au], Stefano Miserocchi[aq], Jürgen Möbius[au], Behzad Mostajir[ai], Laure Mousseau[av], Joan Navarro[l], Nives Ogrinc[aw], Marco Pansera[ax], Silvio Pantoja-Gutiérrez[ay], Vanesa Papiol[az], Constantine Parinos[ac], Catalina Pasqual[y], Alexandra Pavlidou[ac], Rut Pedrosa-Pàmies[ba], John Pinnegar[am], Nicholas V. C. Polunin[bb], Maria Protopapa[ac], Daniel J. Repeta[bc], Nadia Sabatino[bd], Julian P. Sachs[be], Anna Sanchez-Vidal[y], Gianluca Sarà[bf], Nicolas Savoye[ar], Anna Schroeder[w], Ester Skylaki[ac], Daniel M. Sigman[bg], Geraldina Signa[v,bh], Guy Sisma-Ventura[al], Ioanna Stavrakaki[ac], Ulrich Struck[bi], Javier A. Tesán-Onrubia[s,bj,bk], Tommaso Tesi[aq], Sinan Uzundumlu[bl], Maria Valls[o], Salvatrice Vizzini[v,bh], Soultana Zervoudaki[ac], Salem W. Zgozi[bm], Annamaria Zoppini[bn], Barbara Zorica[aj], Trevor J. Willis[c,b]

[a]Department of Earth, Environmental and Life Sciences (DISTAV), University of Genoa, Corso Europa 26, 16132 Genoa, Italy

[b]National Biodiversity Future Center (NBFC), Piazza Marina 61, 90133 Palermo, Italy

[c]Department of Integrative Marine Ecology, Stazione Zoologica Anton Dohrn (SZN-EMI), Fano Marine Center, Viale Adriatico 1N, 61032 Fano (PU), Italy

[d]School of Ocean and Earth Science, University of Southampton, Waterfront Campus, European Way, SO14 3ZH Southampton, United Kingdom

[e]Department of Biological and Environmental Science, University of Jyväskylä, Seminaarinkatu 15, 40014 Jyväskylän yliopisto, Finland

[f]Ifremer, Unité Halieutique Manche Mer du Nord (HMMN), Laboratoire Ressources Halieutiques, F-62200 Boulogne-sur-Mer, France

[g]Centro Oceanográfico de Cádiz, Instituto Español de Oceanografía (COCAD-IEO), Puerto Pesquero, Muelle de Levante s/n, 11006 Cádiz, Spain

[h]Marine and Freshwater Research Center, Atlantic Technological University, H91 T8NW Galway, Ireland

[i]Department of Life and Environmental Sciences (DISVA), Polytechnic University of Marche, Via Brecce Bianche, 60131 Ancona, Italy

[j]Institute for Marine Biological Resources and Biotechnology, National Research Council (CNR-IRBIM), Largo Fiera della Pesca 2, 60125 Ancona, Italy

[k]Institute of Marine Sciences, National Research Council (CNR-ISMAR), Naples, Italy

[l]Renewable Marine Resources, Institut de Ciències del Mar (ICM), CSIC, Passeig Marítim de la Barceloneta, 37-49, 08003 Barcelona, Spain

[m]Norwegian Institute for Nature Research, Fram Center, 9296 Tromsø, Norway

[n]Section of Oceanography, National Institute of Oceanography and Applied Geophysics - OGS, Via Beirut 2, 34151 Trieste, Italy

[o]Oceanographic Center of the Balearic Islands (COB-IEO, CSIC), Moll de Ponent s/n, 07015 Palma, Spain

[p]Institute of Marine Sciences, National Research Council (CNR-ISMAR), Via Piero Gobetti 101, 40129 Bologna, Italy

[q]Institute of Anthropic Impacts and Sustainability in marine environment, National Research Council (CNR-IAS), Lungomare Cristoforo Colombo 4521, 90149 Palermo, Italy

[r]School of Geosciences, University of Edinburgh, The King's Buildings, EH9 3FE Edinburgh, United Kingdom

[s]Aix-Marseille University, University of Toulon, CNRS/INSU, IRD, Mediterranean Institute of Oceanography (MIO), UM 110, 163 avenue de Luminy, 13288 Marseille cedex 09, France

[t]Italian Institute for Environmental Protection and Research (ISPRA), Chioggia, località Brondolo, 30015 Chioggia (VE), Italy

[u]Institute of Anthropic Impacts and Sustainability in marine environment, National Research Council (CNR-IAS), S.S. di Capo Granitola, Via del Mare 3, 91021 Torretta Granitola, Campobello di Mazara (TP), Italy

[v]Department of Earth and Marine Sciences, University of Palermo, Via Archirafi 18, 90123 Palermo, Italy

[w]Institute of Marine Sciences, National Research Council (CNR-ISMAR), Arsenale - Tesa 104, Castello 2737/F, 30122 Venice, Italy

[x]Department of Marine Sciences, Marine Science and Technology Faculty, Çanakkale Onsekiz Mart University, 17020 Çanakkale, Türkiye

[y]GRC Geociències Marines, Departament de Dinàmica de la Terra i de l'Oceà, Universitat de Barcelona, Carrer Martí i Franquès s/n, 08028 Barcelona, Spain

[z]Institute of Marine Sciences, National Research Council (CNR-ISMAR), Area Science Park, Basovizza 10, 34149 Trieste, Italy

[aa]Department of Evolutionary Biology, Ecology and Environmental Science, Faculty of Biology, University of Barcelona, Av. Diagonal 643, 08028 Barcelona, Spain

[ab]Ifremer, Dynamiques des Écosystèmes Côtiers (DYNECO), Laboratory of Coastal Benthic Ecology, F-29280 Plouzané, France

[ac]Institute of Oceanography, Hellenic Center for Marine Research, 46.7 km Athinon-Souniou Avenue, 19013 Anavyssos, Greece

[ad]Section of Oceanography, National Institute of Oceanography and Applied Geophysics - OGS, Via Auguste Piccard 54, 34151 Trieste, Italy

[ae]Sorbonne Université, Laboratoire d'Océanographie Microbienne (LOMIC UMR 7621 CNRS-SU), Observatoire Océanologique de Banyuls, Avenue Pierre Fabre, F-66650 Banyuls-sur-Mer, France

[af]Oceana, 1025 Connecticut Ave NW #200, Washington, DC 20036, USA

[ag]Department of Integrative Marine Ecology, Stazione Zoologica Anton Dohrn (SZN-EMI), Villa Comunale, 80121 Naples, Italy

[ah]Institute of Carbon Cycles, Helmholtz-Zentrum Hereon, Max-Planck-Str. 1, 21502 Geesthacht, Germany

[ai]Marine Biodiversity, Exploitation and Conservation (MARBEC), UMR 9190, CNRS, Université de Montpellier, Ifremer, IRD, Place Eugène Bataillon, Université de Montpellier, Case 93, 34095 Montpellier cedex 05, France

[aj]Laboratory for Fisheries Science, Institute of Oceanography and Fisheries, Šet. I. Meštrovića 63, 21000 Split, Croatia

[ak]National Institute of Oceanography and Applied Geophysics - OGS, Borgo Grotta Gigante 42c, 34010 Sgonico (TS), Italy

[al]National Institute of Oceanography, Israel Oceanographic and Limnological Research, 3102201 Haifa, Israel

[am]Centre for Environment, Fisheries and Aquaculture Science, Lowestoft Laboratory, Pakefield Road, NR33 0HT Lowestoft, United Kingdom

[an]International Council for the Exploration of the Sea, H. C. Andersens Boulevard 44-46, DK 1553 Copenhagen, Denmark

[ao]Institute of Marine Ecosystem and Fishery Science, University of Hamburg, Grosse Elbstrasse 133, 22767 Hamburg, Germany

[ap]Institute of Oceanography, Hellenic Centre for Marine Research, Former American Base of Gournes, 71500 Gournes, Crete, Greece

[aq]Institute of Polar Sciences, National Research Council (CNR-ISP), Via Piero Gobetti 101, 40129 Bologna, Italy

[ar]Université de Bordeaux, CNRS UMR 5805, Bordeaux INP, EPOC, Allée Geoffroy Saint-Hilaire, 33600 Pessac, France

[as]Biology Center of the Czech Academy of Sciences, Institute of Soil Biology and Biogeochemistry, České Budějovice, Czech Republic

[at]University of South Bohemia in České Budějovice, Faculty of Science, České Budějovice, Czech Republic

[au]Institute for Geology, University of Hamburg, Bundesstraße 55, 20146 Hamburg, Germany

[av]Sorbonne Université, Laboratoire d'Océanographie de Villefranche (LOV UMR 7093 CNRS SU), Institut de la Mer de Villefranche, 181 chemin du Lazaret, F-06230 Villefranche-sur-mer, France

[aw]Department of Environmental Sciences, Jožef Stefan Institute, Jamova 39, 1000 Ljubljana, Slovenia

[ax]Sicily Marine Center, Stazione Zoologica Anton Dohrn (SZN), Villa Pace - Contrada Porticatello 29, 98167 Messina, Italy

[ay]Departamento de Oceanografía and Centro de Investigación Oceanográfica COPAS Coastal, Universidad de Concepción, 4070386 Concepción, Chile

[az]Escuela Nacional de Estudios Superiores Mérida, Universidad Nacional Autónoma de México, Tablaje Catastral 6998, Carretera Mérida-Tetiz km 4.5, 97357 Ucú, Yucatán, Mexico

[ba]The Ecosystems Center, Marine Biological Laboratory, 02543 Woods Hole, MA, USA

[bb]School of Natural and Environmental Sciences, Newcastle University, NE1 7RU Newcastle upon Tyne, United Kingdom

[bc]Department of Marine Chemistry and Geochemistry, Woods Hole Oceanographic Institution, 02543 Woods Hole, MA, USA

[bd]Institute of Marine Sciences, National Research Council (CNR-ISMAR), Campus Universitario, Via Archirafi, 90123 Palermo, Italy

[be]School of Oceanography, University of Washington, 98195 Seattle, WA, USA

[bf]Department of Earth and Marine Sciences, University of Palermo, Via delle Scienze Edificio 16, 90128 Palermo, Italy

[bg]Geosciences Princeton University, Bridger Hall, 11 Ivy Lane, 08544 Princeton, NJ, USA

[bh]Consorzio Nazionale Interuniversitario per le Scienze del Mare (CoNISMa), Piazzale Flaminio 9, 00196 Rome, Italy

[bi]Museum für Naturkunde, Leibniz Institute for Evolution and Biodiversity Science, Invalidenstrasse 43, 10115 Berlin, Germany

[bj]Conservatoire National des Arts et Métiers, Institut National des Sciences et Techniques de la Mer, Cherbourg-en-Cotentin, France

[bk]Laboratoire Universitaire des Sciences Appliquées de Cherbourg (LUSAC), Cherbourg-en-Cotentin, France

[bl]Hınıs Vocational School, Department of Medical Services and Techniques, Ataturk University, Erzurum, Türkiye

[bm]Marine Biology Research Center (MBRC), P.O. Box 30830, Tajoura, Libya

[bn]National Research Council, Water Research Institute (CNR-IRSA), Area della Ricerca RM1, 000010 Montelibretti, Rome, Italy

[*]Author for correspondence: sarah.magozzi@unige.it
[†]Deceased

Author name	Email address	ORCiD
Sarah Magozzi[*]	sarah.magozzi@unige.it	0000-0003-4070-9105
Clive N. Trueman	trueman@soton.ac.uk	0000-0002-4995-736X
Matthew R. D. Cobain	matthew.r.d.cobain@jyu.fi	0000-0003-1701-3986
Kirsteen M. MacKenzie	Kirsteen.Mackenzie@ifremer.fr	0000-0003-4045-3445
Katie St. John Glew	katiestjohnglew@gmail.com	0000-0002-0425-1494
José A. Canseco	jantonio.canseco@ieo.csic.es	0000-0002-7712-8649
Eric Díaz-Delgado	eric.diazdelgado@atu.ie	0000-0003-1929-1904
Emanuela Fanelli	e.fanelli@univpm.it	0000-0002-5358-5159
Paola Rumolo	paola.rumolo@cnr.it	0000-0002-1726-1077
Joan E. Cartes	jcartes@icm.csic.es	0000-0002-9465-5264
Boris Espinasse	boris.espinasse@nina.no	0000-0002-7490-5588
Davide Agnetta	dagnetta@ogs.it	0000-0002-3019-9095
Marta Albo-Puigserver	marta.albo@ieo.csic.es	0000-0002-0477-5984
Carme Alomar	carme.alomar@ieo.csic.es	0000-0002-3228-2706
Francesca Alvisi	francesca.alvisi@cnr.it	0000-0003-1256-2257
Fabio Badalamenti	fabio.badalamenti@cnr.it	0000-0002-2395-454X
Daniela Bănaru	daniela.banaru@mio.osupytheas.fr	0000-0002-8126-4328
Daniela Berto	daniela.berto@isprambiente.it	0009-0000-8524-2495
Angelo Bonanno	angelo.bonanno@cnr.it	0000-0002-3868-751X
Chiara Bonaviri	chiabon@libero.it	0000-0002-3897-2361
Lucia Bongiorni	lucia.bongiorni@cnr.it	0000-0001-9033-4992
Yeşim Büyükateş	ybuyukates@comu.edu.tr	0000-0002-4402-4587
Antonio M. Calafat Frau	antonicalafat@ub.edu	0000-0001-7927-3105
Elisa Camatti	elisa.camatti@cnr.it	0000-0002-6934-9759
Carolina Cantoni	carolina.cantoni@cnr.it	0000-0002-3253-1768

Luis Cardona	luis.cardona@ub.edu	0000-0002-7892-1323
Antoine Carlier	Antoine.Carlier@ifremer.fr	0000-0002-1204-4006
Michela Castellano	michela.castellano@unige.it	0000-0001-6101-0112
Spyros Chaikalis†		
Jacopo Chiggiato	jacopo.chiggiato@cnr.it	0000-0002-0998-6473
Tamara Cibic	tcibic@ogs.it	0000-0003-1519- 4891
Pascal Conan†		
Ilaria Conese	ilaria.conese@cnr.it	
Martina Coppari	m.coppari@staff.univpm.it	0000-0002-3178-9409
David Costalago	dcostalago@oceana.org	0000-0003-2224-2222
Pierre Cresson	Pierre.Cresson@ifremer.fr	0000-0002-3485-4261
Isabella D'Ambra	isabella.dambra@szn.it	0000-0001-5486-9535
Kirstin Dähnke	kirstin.daehnke@hereon.de	0000-0001-5133-7082
Audrey M. Darnaude	Audrey.DARNAUDE@cnrs.fr	0000-0001-7129-3902
Salud Deudero	salud.deudero@ieo.csic.es	0000-0001-5584-2801
Daria Ezgeta-Balić	ezgeta@izor.hr	0000-0003-0763-3647
Michele Giani	mgiani@ogs.it	0000-0002-3306-7725
Alexandra Gogou	agogou@hcmr.gr	0000-0001-7327-9223
Gérald Grégori	gerald.gregori@mio.osupytheas.fr	0000-0003-1645-9468
Tamar Guy-Haim	tamar.guy-haim@ocean.org.il	0000-0002-6962-0262
Mireille L. Harmelin-Vivien	mireille.harmelin@mio.osupytheas.fr	0000-0003-3085-2899
Simon Jennings	simon.jennings@ices.dk	0000-0002-2390-7225
Aristomenis P. Karageorgis	ak@hcmr.gr	0000-0003-3910-2541
Rolf Koppelmann	rolf.koppelmann@uni-hamburg.de	0000-0002-0561-9617
Nikolaos Lampadariou	nlamp@hcmr.gr	0000-0003-2171-7150
Leonardo Langone	leonardo.langone@cnr.it	0000-0002-2634-2899
Camilla Liénart	camilla.lienart.pro@gmail.com	0000-0001-5945-9869
Maria Grazia Mazzocchi	grazia.mazzocchi@szn.it	0000-0001-5914-2933
Antonio Mazzola	antonio.mazzola@unipa.it	0000-0001-8433-278X
Travis B. Meador	travis.meador@bc.cas.cz	0000-0001-8255-5883
Louise Merquiol	louise.merquiol@univ-amu.fr	0000-0002-7032-1403
Marc Metzke	marc.metzke@hereon.de	
Stefano Miserocchi	stefano.miserocchi@cnr.it	0000-0002-6315-8919
Jürgen Möbius	maischo@gmx.de	
Behzad Mostajir	behzad.mostajir@umontpellier.fr	0000-0003-4911-794X
Laure Mousseau	laure.mousseau@imev-mer.fr	0009-0000-1747-9909
Joan Navarro	joan@icm.csic.es	0000-0002-5756-9543
Nives Ogrinc	nives.ogrinc@ijs.si	0000-0002-5709-1594
Marco Pansera	marco.pansera@szn.it	0000-0002-2784-9931
Silvio Pantoja-Gutiérrez	spantoja@udec.cl	0000-0001-8225-7624
Vanesa Papiol	vpapioln@gmail.com	0000-0001-6891-0148

Constantine Parinos	ksparinos@hcmr.gr	0000-0002-7700-374X
Catalina Pasqual	catalinapmas@gmail.com	0000-0001-8657-327X
Alexandra Pavlidou	aleka@hcmr.gr	0000-0002-0031-4726
Rut Pedrosa-Pàmies	rpedrosa@mbl.edu	0000-0003-3504-4727
John Pinnegar	john.pinnegar@cefas.co.uk	0000-0001-5061-9520
Nicholas V. C. Polunin	nick.polunin@ncl.ac.uk	0000-0002-1480-8794
Maria Protopapa	mariaprot@hcmr.gr	0000-0002-9030-1469
Daniel J. Repeta	drepeta@whoi.edu	0000-0003-1927-0599
Nadia Sabatino	nadia.sabatino@cnr.it	0009-0000-5646-7759
Julian P. Sachs	jsachs@uw.edu	0000-0002-6247-9286
Anna Sanchez-Vidal	anna.sanchez@ub.edu	0000-0002-8209-1959
Gianluca Sarà	gianluca.sara@unipa.it	0000-0002-7658-5274
Nicolas Savoye	nicolas.savoye@u-bordeaux.fr	0000-0001-6433-8519
Anna Schroeder	anna.schroeder@cnr.it	0000-0002-7389-6907
Ester Skylaki	e.skylaki@hcmr.gr	0009-0009-1497-7625
Daniel M. Sigman	sigman@princeton.edu	0000-0002-7923-1973
Geraldina Signa	geraldina.signa@unipa.it	0000-0003-2171-3299
Guy Sisma-Ventura	guy.siv@ocean.org.il	0000-0002-6962-0262
Ioanna Stavrakaki	istavrakaki@hcmr.gr	0009-0006-9830-5508
Ulrich Struck	ulrich.struck@mfn.berlin	0000-0001-8563-099X
Javier A. Tesán-Onrubia	tesan.onrubia@gmail.com	0000-0002-2276-6408
Tommaso Tesi	tommaso.tesi@cnr.it	0000-0002-1686-3375
Sinan Uzundumlu	sinan.uzundumlu@atauni.edu.tr	0000-0003-0366-9116
Maria Valls	maria.valls@ieo.csic.es	0000-0001-9070-8181
Salvatrice Vizzini	salvatrice.vizzini@unipa.it	0000-0002-7127-7555
Soultana Zervoudaki	tanya@hcmr.gr	0000-0002-3499-8433
Salem W. Zgozi	Salemzgozi60@gmail.com	
Annamaria Zoppini	annamaria.zoppini@irsa.cnr.it	0000-0003-2474-5173
Barbara Zorica	zorica@izor.hr	0000-0002-9131-4675
Trevor J. Willis	trevor.willis@szn.it	0000-0002-0357-1189

Abstract

Isoscapes – spatial models of stable isotope ratios – are powerful tools for understanding biogeochemical cycles, food web structure, and ecological connectivity. In marine systems, however, broad-scale isoscapes are difficult to constrain because reference datasets are typically heterogeneous and opportunistic. Bayesian hierarchical models implemented through Integrated Nested Laplace Approximation (INLA) provide an efficient framework for modeling spatial patterns while accounting for non-spatial variance. We tested whether broad-scale geographic baseline isoscapes could be constrained for the Mediterranean Sea using INLA models applied to an opportunistically compiled dataset from this semi-enclosed basin, where strong environmental gradients are expected but spatially explicit baselines remain lacking. We assembled the most comprehensive dataset of $\delta^{13}C$ and $\delta^{15}N$ values to date for low-trophic-level, primarily epipelagic food web compartments (>6,000

samples from >600 sites). Although discrete regions of relatively high and low δ values were identified, particularly for $\delta^{15}N$, semivariograms and model outputs indicated only short-range spatial autocorrelation (ca. 40 km for $\delta^{13}C$; 65 km for $\delta^{15}N$) within this large dataset. Environmental covariates improved model fit for $\delta^{15}N$ values but did not enhance predictive performance or alter spatial predictions. Our results demonstrate that even advanced spatial models may not compensate where sampling design is structurally mismatched relative to unknown but structured spatial and non-spatial sources of isotopic variation. Coordinated sampling designed to capture spatial variability while accounting for major sources of non-spatial variance is required to develop robust marine isoscapes supporting ecological and management applications in the Mediterranean Sea and similar regions.

Keywords

isoscapes, stable isotopes, spatial modeling, Bayesian inference, opportunistic datasets, sampling design, Mediterranean Sea

Highlights

- >6,000 isotope samples compiled across the Mediterranean Sea
- Differences exists among well-sampled regions but do not scale across the basin
- INLA models cannot separate spatial and non-spatial variance
- Unstructured sampling obscures spatial isotope patterns
- Coordinated sampling is required for robust marine isoscapes

1 Introduction

Stable isotope ratios of elements often vary systematically across environments due to biogeochemical and physical processes [1]. These spatial patterns can be expressed as isoscapes – mechanistic or statistical models that explicitly predict isotopic variation across space [1, 2]. Mechanistic models predict spatial patterns from underlying physical and biogeochemical processes, whereas statistical models infer spatial patterns directly from observed data. Isoscapes provide valuable insight into biogeochemical processes [3–6] and have broad applications in spatial ecology [7–10], trophic ecology [11–14], and forensic traceability [15–18].

In marine environments, isoscape development has traditionally lagged behind terrestrial systems due to the logistical challenges of obtaining reference samples at appropriate spatial and temporal scales [19, 20]. Mechanistic models can partly overcome these limitations by predicting isotopic variation from first principles [19, 21], but sample-based statistical isoscapes remain essential in systems where spatial isotope patterns emerge from multiple interacting processes that are difficult to resolve mechanistically.

Statistical isoscapes of carbon, nitrogen, and sulfur have been developed for several oceanic regions [8, 22–27], offering opportunities for research and management at regional to basin scales. These isoscapes are typically generated by spatially interpolating measured isotope values based on geographic distance [7, 8], relationships with environmental covariates [28, 29], or both [23]. Ideally, reference samples are obtained through targeted, gridded sampling (e.g., [8]) designed to capture spatially structured variation. In practice, however, most broad-scale marine isoscapes rely on opportunistically collected data, particularly for offshore or logistically challenging regions [22, 25–27]. Such datasets are often unevenly distributed in space and heterogeneous with respect to time

periods, depths, taxa, and analytical methods. This heterogeneity introduces non-spatial sources of isotopic variability – arising from temporal (seasonal to decadal scales; e.g., [27, 30–34]), vertical [35–40], and biological [41–44] processes – that can confound spatial patterns. As a result, when sampling is not structured relative to these sources of variation, underlying geographic signals may be obscured or difficult to resolve [24].

The increasing availability of compiled isotope datasets (e.g., [45–48]) creates new opportunities to develop isoscapes. Addressing this challenge requires statistical approaches capable of partitioning variance into spatial and non-spatial components, allowing genuine geographic structure to be distinguished from variation arising from opportunistic data compilation (e.g., time periods, depths, taxa, sizes, trophic levels, methods). Bayesian hierarchical models implemented through Integrated Nested Laplace Approximation (INLA) provide an efficient and flexible framework for spatial modeling while accounting for systematic non-spatial variance, provided that spatial coverage is sufficient and that key sources of non-spatial variation can be constrained [24, 26, 27]. INLA-based methods therefore offer a means to test whether spatial variance can be reliably extracted from opportunistic datasets, and under what conditions spatial and non-spatial sources of variance can be distinguished. This is a question of broad relevance for large-scale marine isoscape development.

1.2 The Mediterranean Sea test case

The Mediterranean Sea is an ideal candidate for isoscape development. The region holds major ecological, economic, and geopolitical significance but faces intense anthropogenic pressure from coastal development, pollution, habitat degradation, and overfishing [49–52], with many fish stocks already overexploited [53]. Rapid warming [54–57] and pronounced tropicalization in the eastern basin [58–60] are reshaping community structure and ecosystem functioning. Lessepsian migrations through the Suez Canal continue to introduce non-indigenous species, further altering Mediterranean food webs [61–63]. These ecological changes occur within a fragmented governance framework that complicates coordinated management and conservation [64].

Stable isotope analyses have long been applied to ecological and biogeochemical studies in the Mediterranean, yet most applications remain geographically restricted and locally focused. Developing basin-scale isoscapes would provide a unifying, spatially explicit framework to integrate these diverse efforts, enabling isotopic data to be interpreted consistently across broader geographic contexts. In turn, this would enhance the capacity of isotope data to inform ecosystem-based management and spatial planning under accelerating environmental change. Table 1 summarizes key Mediterranean applications of stable isotopes that would directly benefit from spatialization through isoscapes.

Table 1. Summary of key stable isotope applications in the Mediterranean Sea that would benefit from spatialization through isoscapes, encompassing biogeochemical, ecological, and applied management contexts. Isoscapes provide spatially explicit baseline information that supports consistent, basin-scale interpretation of isotopic data and facilitates the integration of local studies. Where available, examples of isoscape-based analyses are provided.

Biogeochemistry	**Trophic Ecology**	**Spatial/Movement Ecology**	**Applied Ecosystem Management and Forensics**
Constraining the balance of N_2 fixation vs terrestrial/anthropogenic nitrogen inputs in the Mediterranean Sea [65–69]	Establishing isotopic baselines for spatial inference of trophic geography and structure [12–14, 45] and for the parameterization isotope mixing models, niche analyses, and assessments of trophic interactions [37, 85–90]	Providing natural georeferenced tags to complement artificial tagging [8, 20, 22]; isoscapes remove the need for directed georeferenced sampling of target species in all possible origin regions [108, 109]	Contributing to monitoring frameworks (e.g., MSFD; [46, 120–123])
Testing and refining isotope-enabled biogeochemical models [3, 21] to improve reconstructions of past [4, 70, 71] and projections of future nutrient dynamics [5, 6]	Accounting for isotopic variation in food web models introduced by mobile consumers transporting organic matter across habitats or trophic levels [91, 92]	Coupling with agent-based models [10, 110], tagging data [7, 111, 112] or oceanographic models [113] to improve movement reconstruction accuracy and identify feeding hotspots	Optimizing placement and evaluating effectiveness of MPAs [124–126]
Evaluating biogeochemical consequences of deep-water mass formation and its temporal/spatial variability	Informing and testing ecosystem models, facilitating development of isotope-enabled food web models [93–97]	Quantifying functional connectivity [114, 115]	Testing claims of geographic origin of seafood and marine products (e.g., combatting IUU fishing and food fraud, and enhancing regional product protection) [16, 17]
Quantifying the proportional contributions of different organic matter sources, including terrestrial and riverine inputs, particularly across coastal-offshore and land-sea gradients [68, 72–77]	Tracing nutrient fluxes through food webs across habitats and depth layers, including land-sea interfaces [98–100], vertical transfers [36, 38, 101–103], and benthic-pelagic coupling [104–107]	Identifying routes for pathogen transport via migratory species	Supporting isotope applications in fisheries management [127–130]
Tracing the entry and dispersion of anthropogenic nutrient pollutants [78–84]		Enabling retrospective analyses from archived biological materials [10, 116]	Supporting interpretations of fundamental ecological data for data-deficient and high-conservation-concern species (turtles, seabirds, cetaceans, elasmobranchs; non-lethal sampling) [7, 9, 13, 113, 131, 132]
		Investigate spatial aspects and comparisons of biological invasions [117–119]	

The Mediterranean Sea consists of two deep basins with restricted circulation and deep-water exchange. It exhibits pronounced biogeochemical and climatic gradients: temperature and salinity increase eastward, while nutrient availability and productivity decrease [50, 133–136]. North-to-south gradients within both basins further reflect decreasing nutrient concentrations and productivity alongside increasing temperature and salinity. These environmental contrasts are expected to generate systematic isotopic variation in pelagic surface primary production, producing predictable $\delta^{13}C$ and $\delta^{15}N$ gradients in macronutrients and low-trophic-level food web compartments. For carbon, isotopic variability arises primarily from fractionation during photosynthesis [137–139], which depends on the carbon demand-to-supply ratio in phytoplankton and is therefore influenced by CO_2 availability, phytoplankton growth rate, and temperature [138–141]. Consequently, longitudinal gradients in CO_2 concentration, nutrient availability, productivity, and temperature are expected to produce broad west-to-east differences in phytoplankton $\delta^{13}C$ values, as demonstrated in other marine regions [24, 26]. For nitrogen, spatial patterns in $\delta^{15}N$ values reflect variation in nitrogen sources and utilization [142]: in oligotrophic eastern regions, enhanced N_2 fixation and atmospheric deposition are expected to introduce isotopically lighter nitrogen [65, 69, 143–145], whereas in the more productive western regions, greater anthropogenic and terrestrial nitrogen inputs contribute ^{15}N-enriched nitrate. In contrast, deep-water gradients are likely to be subtler, reflecting the basin's relatively stable physical structure at depth and the combined influences of remineralization, mixing, and deep-water formation [39, 40, 146].

Despite these expected gradients, no basin-scale isoscapes have yet been developed for the Mediterranean Sea. This reflects both the lack of spatially representative reference datasets for statistical modeling and the challenges of mechanistically modeling semi-enclosed basins with complex circulation dynamics [19, 21]. However, the extensive collection of local and regional isotope datasets provides an opportunity to construct a spatially broad, albeit heterogeneous, compiled reference dataset. Here, we leverage this opportunity and use the Mediterranean Sea as a test case to evaluate the feasibility of developing broad-scale geographic baseline isoscapes from opportunistically compiled data. We assembled a comprehensive reference dataset integrating available $\delta^{13}C$ and $\delta^{15}N$ records from diverse sample types representing low-trophic-level compartments of food webs primarily fueled by epipelagic production. We then applied INLA models to test whether broad-scale isotopic gradients can be resolved from such data, and to assess the extent to which spatial structure can be distinguished from non-spatial sources of variation. Our aim is therefore not only to develop a Mediterranean isoscape, but also to evaluate how sampling design influences the ability to recover spatial patterns in isotopic data. In particular, we focus on cases where sampling is not structured to capture spatial variability, and where additional heterogeneity in sampling conditions may further obscure underlying spatial signals. Ultimately, our goal is to identify the conditions under which isoscape models can provide robust spatial inference, and to inform future sampling strategies in the Mediterranean Sea and other complex marine systems.

2 Materials and Methods

2.1 Data compilation

To develop isoscapes, we compiled all available georeferenced $\delta^{13}C$ and $\delta^{15}N$ data from published and unpublished studies in the Mediterranean region. During data compilation, it became clear that the resulting dataset would unevenly be distributed in space and heterogeneous with respect to sample types, metadata, and sampling conditions, and therefore not appropriately structured relative to expected underlying sources of isotopic variation. Constructing a usable reference dataset under these conditions requires a tradeoff between restricting inclusion to well-documented samples with standardized metadata, and maximizing spatial coverage while accepting greater uncertainty [24]. As

isoscape models require geographically extensive datasets to resolve spatial gradients, we opted for the latter and prioritized spatial coverage.

The compiled dataset included a broad range of sample types, each functionally representative – to varying degrees – of low-trophic-level compartments of marine food webs primarily sustained by epipelagic or pelagic production (Tables S.1 and S.2). Given inconsistencies in metadata structure, completeness, and granularity across sources, we classified samples into six broad ecological categories: pico-nanoplankton, phytoplankton, particulate organic matter (POM), zooplankton, suprabenthos, and sediment, following study-specific categorizations when available. Our category 'pico-nanoplankton' corresponded to the <20 µm fraction, 'phytoplankton' to identified phytoplankton and/or the 20-200 µm fraction, and 'POM' to samples described as bulk particulate organic material or broad size fractions (<200 µm), with distinction between suspended and sinking material retained where available. The 'zooplankton' category included bulk, size-fractionated, or taxonomically resolved samples depending on data availability, with size and taxonomic information retained where provided. 'Suprabenthos' included assemblages or taxa consistent with suprabenthic ecology, such as caridean and penaeoid decapods, amphipods, isopods, and mysids. 'Sediment' samples corresponded to surface sediments or upper sedimentary layers (typically ≤0.5 cm). More detailed category descriptions, size classes, and taxonomic levels are provided in Tables S.1 and S.2. Sample categories were defined to maximize within-group comparability and expected between-group differences while retaining sufficient sample sizes for modeling. This classification provided a pragmatic framework for partitioning variance, enabling the full dataset to be used to model spatial isotope structure while explicitly accounting for systematic differences among categories. We included sediment samples as a category despite remineralization processes, as surface sediment organic matter retains a largely epipelagic origin [74, 75, 147]. Similarly, suprabenthic organisms remain closely linked to pelagic production despite interacting with benthic systems [36, 101, 148]. Only minimal exclusion criteria were applied *a priori*. We excluded samples that did *not* represent low-trophic-level compartments fueled by pelagic production, including riverine particulate organic matter, sediment cores (affected by diagenetic alteration), strictly benthic infaunal organisms, and higher-trophic-level consumers with carnivorous diets (e.g., cephalopods, teleosts, and elasmobranchs). Individual baseline samples with $\delta^{13}C$ and/or $\delta^{15}N$ values outside plausible bulk marine environmental ranges (-40 to -10‰ and -5 to 15‰ for $\delta^{13}C$ and $\delta^{15}N$, respectively) were excluded. Samples from very nearshore locations were excluded during model construction, as environmental covariate data were unavailable at those sites given the spatial extent and resolution of the covariate layers (Table S.3).

2.2 Environmental covariates

Environmental variables previously shown to correlate with $\delta^{15}N$ and $\delta^{13}C$ values (e.g., [23, 24, 27, 28, 149]) and varying across broad spatial gradients in the Mediterranean Sea were selected for the models. Environmental data encompassing both physical and biogeochemical variables were obtained from the Copernicus Monitoring Environment Marine Service [150], with monthly averages available at 0.042° x 0.042° spatial resolution for the period 2009-2019. Physical variables – sea surface temperature (SST), bottom temperature (BT), sea surface salinity (Sal), mixed layer depth (MLD), and bathymetry (Bathy) – were extracted from the Mediterranean Sea Physics Reanalysis product (MEDITERRANEAN SEA_MULTIYEAR_PHY_006_004; [151]). Biogeochemical variables – chlorophyll *a* concentration (Chl), phytoplankton biomass (phytoC), primary production (PP), and concentrations of nitrate (NO_3^-), phosphate (PO_4^{3-}), ammonium (NH_4^+), and dissolved inorganic carbon (DIC) – were obtained from the coupled Mediterranean Sea Biogeochemistry Reanalysis model (MEDITERRANEAN SEA_MULTIYEAR_BGC_006_008; [152]).

We used model-derived climatologies rather than observational (e.g., satellite) datasets for three main reasons. First, satellite products are unavailable for several variables relevant to isotope dynamics (e.g., DIC, nutrients, bottom temperature). Second, model outputs provide internally consistent fields for both physical and biogeochemical variables at matching spatial and temporal resolutions. Third, the CMEMS Reanalysis products used here have been validated against extensive *in situ*, satellite, and climatological observations and show good performance at basin scales [151, 152]. For example, physical variables show strong agreement with observations (e.g., RMSD ca. 0.55 °C for SST; ca. 0.17-0.18 PSU for Sal), while biogeochemical variables effectively reproduce basin-scale distributions and variability (e.g., RMSD ca. 0.04 mg m^{-3} for Chl in open waters; ca. 0.07-0.19 mg m^{-3} for NO_3^- across depth layers). Model-derived climatologies therefore capture large-scale spatial gradients and vertical structure across the Mediterranean Sea, although uncertainties increase at finer spatial and temporal scales. This approach ensures spatial and temporal coherence among covariates while maintaining ecological relevance across a broad suite of variables. For integrated surface values, monthly values for each variable were averaged across depths shallower than 40 m, corresponding to the lower limit of the seasonal thermocline in the Mediterranean Sea [153, 154]. Monthly climatologies were then computed across years (2009-2019), from which annual averages were derived.

In addition to environmental variables, we included the spatially derived least-cost distance to coast (dCoast) as an additional covariate. This was computed from each grid cell to the nearest coastline using a binary cost surface, where movement through sea cells had low and equal cost (conductance = 1), while land was treated as an impassible barrier (conductance = 0). The cost surface was generated from a raster at the same resolution as the modeled climatologies, and distance calculations were performed using the *gdistance* R package [155]. This metric captures the complex coastal and island geography of the Mediterranean Sea and provides a more realistic representation of marine connectivity than straight-line (Euclidean) distance.

For spatial prediction, we created a regular 50 km resolution grid based on a custom Lambert Azimuthal Equal-Area (LAEA) projection centered on the Mediterranean Sea, covering the domain from -4° to 39.5° longitude and from 27.5° to 44.5° latitude. Covariate values were extracted at each grid point. To avoid extrapolation beyond the range of observed environmental conditions, we excluded prediction points with missing covariate values or with values falling outside 5% of the observed range at sample locations. All covariates were mean-centered prior to modeling (see Fig. S.5 for maps of individual environmental variables).

2.3 Sample variograms

To independently assess spatial autocorrelation in the reference samples, we computed empirical semivariograms for $\delta^{13}C$ and $\delta^{15}N$ values [156]. Instead of Euclidean distances, we used least-cost distances between sample locations, calculated using the same approach as for dCoast described above. Semivariograms were generated using 100 evenly spaced distance bins from 0 to 4000 km, retaining only bins containing ≥500 sample pairs to ensure robust estimates.

To compare basin-scale spatial autocorrelation patterns with those in areas characterized by denser and more spatially uniform sampling, we also computed semivariograms for three subregions: the Adriatic Sea, Gulf of Lion, and Balearic Sea. Bin widths were adjusted to 22.5, 6.25, and 8.75 km, respectively, to reflect the smaller spatial extent of these subregions while maintaining sufficient sample support (≥100 pairs per bin).

While INLA-based models explicitly account for non-spatial, category-level differences via random effects, semivariograms were computed using all reference samples pooled across categories. As a result, estimates of spatial autocorrelation may be confounded by between-category variation. Category-specific semivariograms were not feasible due to limited spatial coverage within individual categories. Consequently, semivariograms reflect both spatial structure and the sampling structure of categories. Because categories differ in spatial clustering and coverage, short-distance bins may be dominated by within-category comparisons, whereas larger distance bins may increasingly include between-category comparisons.

2.4 INLA models

To construct isoscape models, we used a Bayesian hierarchical spatial modeling framework implemented through the INLA method via the *R-INLA* package [157, 158]. This approach allows environmental covariates to be included as linear fixed effects, and both spatial (via a latent Gaussian Markov Random Field; hereafter spatial field) and nominally non-spatial (e.g., categorical groupings) factors are modeled as random effects. The application of INLA to isoscape modeling is described in detail by St John Glew et al. [24]; here we summarize only the elements specific to this study.

INLA enables flexible modeling of spatial fields using a Delaunay triangulated mesh that accounts for boundary effects (i.e., land; Fig. S.7). Observation locations served as the initial mesh vertices, with additional vertices added to optimize triangle size while maintaining higher resolution in areas with denser sampling. To capture broad-scale spatial structure but avoid interpolation artefacts, the maximum triangle edge length was set to 100 km.

Each isotope value was modeled as a function of covariates (where included), sample category, and a spatial field (Eq. 1):

$$
\begin{aligned}
&Y_i \sim Intercept + \beta_i X_i + f(U_i) + f(W_i) + \varepsilon_i, \\
&U_i \sim N(0, \sigma^2_{\text{category}}), \\
&W_i \sim N(0, \Omega), \\
&\varepsilon_i \sim N(0, \sigma^2)
\end{aligned} \tag{1}
$$

where Y_i is the isotope value ($\delta^{15}N$ or $\delta^{13}C$) at location i, X_i is a vector of covariates with associated coefficients β_i, U_i is the category random effect, W_i represents the spatial field (with Matérn covariance Ω), and ε_i is the independent residual.

In addition to linear fixed effects, covariates were also modeled as smooth terms. Smooth terms were constructed as second-order basis splines using a 1D mesh and corresponding projection (A) matrix, specifying nine equally distributed knots to capture potential non-linear patterns while minimizing the risk of overfitting. Smooth terms were preferred over interaction terms due to their flexibility, which improves predictive performance and facilitates the emergence of non-linear relationships. Non-informative default priors were applied throughout.

We tested a suite of INLA models combining linear or smooth covariates, sample category, and spatial structure, along with null models that included only spatial and category random effects. Model selection was based primarily on Watanabe-Akaike Information Criteria (WAIC), complemented by evaluation of predictive performance (Pearson correlation between observed and fitted values), and posterior estimates of the spatial field's range (spatial autocorrelation) and variance. Using the selected models, we predicted isotope values at the mesh vertices. These

predictions were interpolated across mesh triangles using a second-order (quadratic) basis function via Bayesian kriging to generate spatially continuous isoscapes. For each grid cell, we extracted mean and variance predictions to map the expected isotopic composition and associated uncertainty of low-trophic-level compartments of marine food webs primarily fueled by epipelagic production across the Mediterranean Sea.

2.4.1 Covariate and Random Effect structure

Preliminary model testing was conducted to identify the most appropriate covariate set and random-effect structure for subsequent comparisons among null, linear, and smooth models, and for isoscape prediction. For covariate selection, environmental variables we first assessed for collinearity using pairwise correlations and variance inflation factors (VIFs). Collinear variables were then summarized using principal component analysis based on values extracted at each sample location, including temperature (SST), productivity (Chl, phytoC, and PP), and nutrients (NO_3^-, PO_4^{3-}, and NH_4^+). The first principal component (PC1) explained >80% of the variance and represented a broad west-to-east gradient of increasing temperature and decreasing nutrients and productivity. PC2 explained only 7-8% (for $\delta^{15}N$ and $\delta^{13}C$, respectively) of the variance and primarily captured finer-scale nutrient contrasts (see Fig. S.6 for PCA of full set of environmental variables). Despite its limited contribution to total variance, PC2 was retained for testing to assess potential improvement in model performance. We also compared alternative variables among other collinear pairs (DIC vs Sal, Bathy vs dCoast). Non-collinear variables (BT, MLD) and PC1 were retained in all models. The final covariate set used in model comparisons included BT, MLD, PC1, DIC, and Bathy.

To evaluate random-effect structure, we tested alternative groupings of isotopically similar or ecologically related categories (e.g., combining pico-nanoplankton and POM, and phytoplankton and POM based on expected partial overlap between size fractions; and combining pico-nanoplankton and sediment based on observed $\delta^{13}C$ similarity). We also explored reduced dataset configurations (e.g., excluding suprabenthos or retaining only POM without a category effect). In addition, we tested the inclusion of season and year as additional random effects using both crossed (Category + Season; Category + Year) and nested (Season within Category) structures in restricted datasets with complete temporal metadata. Across all tests, these alternative structures did not improve predictive performance, spatial structure, or interpretability. For completeness, Category + Season models are reported for comparison. Subsequent analyses therefore focus on the most parsimonious and informative structure, including category as the sole random effect with all six category levels and the full dataset.

3 Results

3.1 The Mediterranean Sea reference dataset

The compiled dataset comprised 5,428 samples from 595 locations for $\delta^{15}N$ and 6,034 samples from 610 locations for $\delta^{13}C$ across the Mediterranean Sea (Tables S.1 and S.2). Despite its size, spatial coverage was highly uneven. Sampling density was highest in the Gulf of Lion and Balearic Sea, moderate in the Adriatic, Ionian, and Aegean-Cretan Seas, and sparse in the southern and southeastern Mediterranean, particularly in the southern Levantine Basin (Fig. 1, S.2A, B).

The distribution of sample categories also varied spatially (Fig. 1, S.2C, D). POM and zooplankton accounted for over 75% of samples in most areas, although their relative contributions differed regionally. Zooplankton dominated datasets from the Adriatic (58-65% for $\delta^{13}C$ and $\delta^{15}N$), Ligurian (60-63% for $\delta^{15}N$ and $\delta^{13}C$), and Balearic Seas (52-55% for $\delta^{13}C$ and $\delta^{15}N$), whereas POM was most

prevalent in the Aegean Sea (91-95% for $\delta^{15}N$ and $\delta^{13}C$) and eastern Mediterranean (0.53-64% for $\delta^{15}N$ and $\delta^{13}C$). Pico-nanoplankton, phytoplankton, suprabenthos, and sediment were less frequently sampled and more unevenly distributed. Sediment samples were more common in the Tyrrhenian (16-17% for $\delta^{13}C$ and $\delta^{15}N$), Adriatic (19-27% for $\delta^{15}N$ and $\delta^{13}C$), and Ionian Seas (3-19% for $\delta^{13}C$ and $\delta^{15}N$); pico-nanoplankton and phytoplankton were concentrated in the Ligurian Sea (17-18% for $\delta^{15}N$ and $\delta^{13}C$); and suprabenthos was represented only in the western Mediterranean (2-3% for $\delta^{15}N$ and $\delta^{13}C$) and Balearic (20-22% for $\delta^{13}C$ and $\delta^{15}N$) and Ionian Seas (22-30% for $\delta^{15}N$ and $\delta^{13}C$).

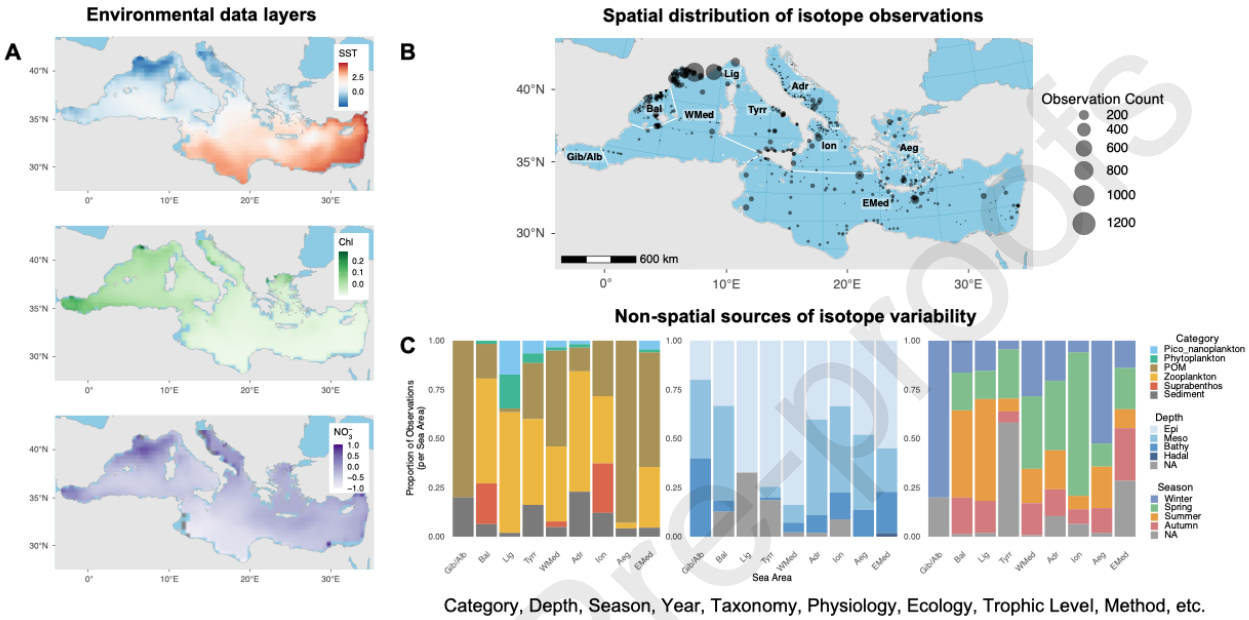

Figure 1. Conceptual overview of the main data inputs for INLA models: environmental data layers (A), spatial distribution of isotope observations (B), and non-spatial sources of isotope variability (C). Panel A shows three example environmental layers – sea surface temperature (SST [°C]), chlorophyll *a* concentration (Chl [mg m^{-3}]), and nitrate concentration (NO_3^- [mmol m^{-3}]) – illustrating basin-scale gradients in temperature, productivity, and nutrient availability across the the Mediterranean Sea. Covariates are shown as mean-centered annual averages of multi-year climatologies. Additional environmental variables and principal component analyses are presented in Fig. S.5 and S.6. Panel B shows sampling locations of isotope observations, with circle size proportional to the number of observations per location. International Hydrographic Organization (IHO) sea area boundaries are indicated (Gib/Alb = Strait of Gibraltar/Alboran Sea, Bal = Balearic Sea, Lig = Ligurian Sea, Tyrr = Tyrrhenian Sea, NWMed = North-Western Mediterranean Sea, Adr = Adriatic Sea, Ion = Ionian Sea, Aeg = Aegean Sea, EMed = Eastern Mediterranean See; see Fig. S.1). Observations are pooled across $\delta^{15}N$ and $\delta^{13}C$; isotope-specific distributions are shown in Fig. S.2A, B. Panel C shows the proportional representation of category, depth zone, and season across IHO sea areas, based on pooled observations. Isotope-specific proportions are provided in Fig. S.2C, D (category), S.3 (depth), and S.4 (season). Additional sources of isotopic variability include year, taxonomy, biological and ecological traits, trophic structure, and sampling and analytical methods.

Vertical and seasonal sampling structure varied among sea areas and categories. Approximately 61-66% of samples (for $\delta^{15}N$ and $\delta^{13}C$, respectively) were collected from epipelagic depths (<200 m), primarily comprising pico-nanoplankton, phytoplankton, POM, and zooplankton (Fig. S.3). Deeper samples contributed 21-23% ($\delta^{13}C$ and $\delta^{15}N$) from mesopelagic, 8-10% ($\delta^{13}C$ and $\delta^{15}N$) from bathypelagic, and <1% (both isotopes) from hadal depths, and were mainly represented by POM, zooplankton, and sediment in the Balearic, Adriatic, Ionian and Aegean Seas, as well as in the eastern Mediterranean. Suprabenthos samples originated primarily from mesopelagic depths.

Total sampling period spanned from October 1993 to March 2022 for $\delta^{15}N$ and from July 1995 to March 2022 for $\delta^{13}C$. Seasonal coverage was uneven across sea areas and categories, with many category x season combinations underrepresented or absent (Fig. S.4). Metadata on depth, year, and season were frequently incomplete or inconsistently reported. Together, these patterns highlight the uneven and heterogeneous structure of the reference dataset.

3.2 Isotopic variability in the Mediterranean Sea

Values of $\delta^{15}N$ in the reference dataset had a mean ± SD of 3.6 ± 2.3‰, with 95% of values ranging from -1.1 to 8.4‰. Values of $\delta^{13}C$ had a mean ± SD of -22.6 ± 2.7‰, spanning a 95% interval from -27.3 to -15.7‰. Within-category variability (red diagonal values in Table S.4) ranged between 0.4 and 1.9‰ (mean SD) for $\delta^{15}N$ and between 0.2 and 1.7‰ for $\delta^{13}C$. Sediment exhibited the lowest variability for both isotopes, whereas pico-nanoplankton and suprabenthos showed the highest variability for $\delta^{15}N$ and $\delta^{13}C$, respectively. Overall, $\delta^{15}N$ values showed slightly greater variability than $\delta^{13}C$ values, except in phytoplankton and suprabenthos.

Between-category mean absolute differences (black off-diagonal values in Table S.4) ranged from 0.3 to 3.5‰ for $\delta^{15}N$ and from 0.1 to 4.1‰ for $\delta^{13}C$. On average, sediment was enriched in ^{15}N by 0.3‰ relative to POM (the smallest difference), while suprabenthos was enriched by 3.5‰ relative to sediment (the largest). Zooplankton was also ^{15}N-enriched by 3.2‰ compared to pico-nanoplankton but unexpectedly depleted by 2.7‰ relative to phytoplankton. For $\delta^{13}C$, the smallest difference (0.1‰) was between zooplankton and sediment, with zooplankton slightly enriched in ^{13}C relative to sediment. The largest difference (4.1‰) occurred between sediment and phytoplankton, with phytoplankton enriched relative to sediment. Zooplankton was ^{13}C-enriched relative to both POM (2.2‰) and pico-nanoplankton (2.1‰). Overall, between-category differences were often comparable in magnitude to within-category variability.

3.3 Sample variograms

Least-cost distance semivariograms showed that category-pooled variance in both $\delta^{15}N$ and $\delta^{13}C$ values increased sharply at small spatial scales (within a few hundred kilometers; Fig. 2). For $\delta^{15}N$, semivariance increased steeply within the first 250 km, continued to increase until ca. 600 km, and then fluctuated inconsistently thereafter (Fig. 2A). The $\delta^{13}C$ semivariogram showed a similarly steep increase within the first 250 km until ca. 750 km, followed by a noisy plateau and a marked decrease between ca. 1,600 and 2,000 km (Fig. 2B). Spatial autocorrelation in both isotopes was therefore limited to short distances – on the order of a few hundred kilometers or less – beyond which isotope values became statistically independent. Subregional semivariograms exhibited similarly weak or shorter-range spatial autocorrelation than at the basin scale (Fig. S.8), with some regions showing no detectable autocorrelation. This indicates that small-scale variability persisted even in regions with denser and more spatially uniform sampling.

Because semivariograms were computed across pooled categories, these patterns reflect both spatial structure and differences in sampling among categories. Categories differed markedly in spatial support, with mean nearest-neighbor least-cost distance ranging from 12.5-12.7 km (for $\delta^{15}N$ and $\delta^{13}C$, respectively) for suprabenthos to 138.5-144.5 km (for $\delta^{13}C$ and $\delta^{15}N$) for pico-nanoplankton. As a result, short-distance bins are dominated by comparisons among spatially clustered samples within categories, whereas comparisons at larger distances increasingly include samples from more spatially dispersed categories and between-category contrasts. Consequently, semivariance reflects a mixture of spatial and category-related variability that varies with distance.

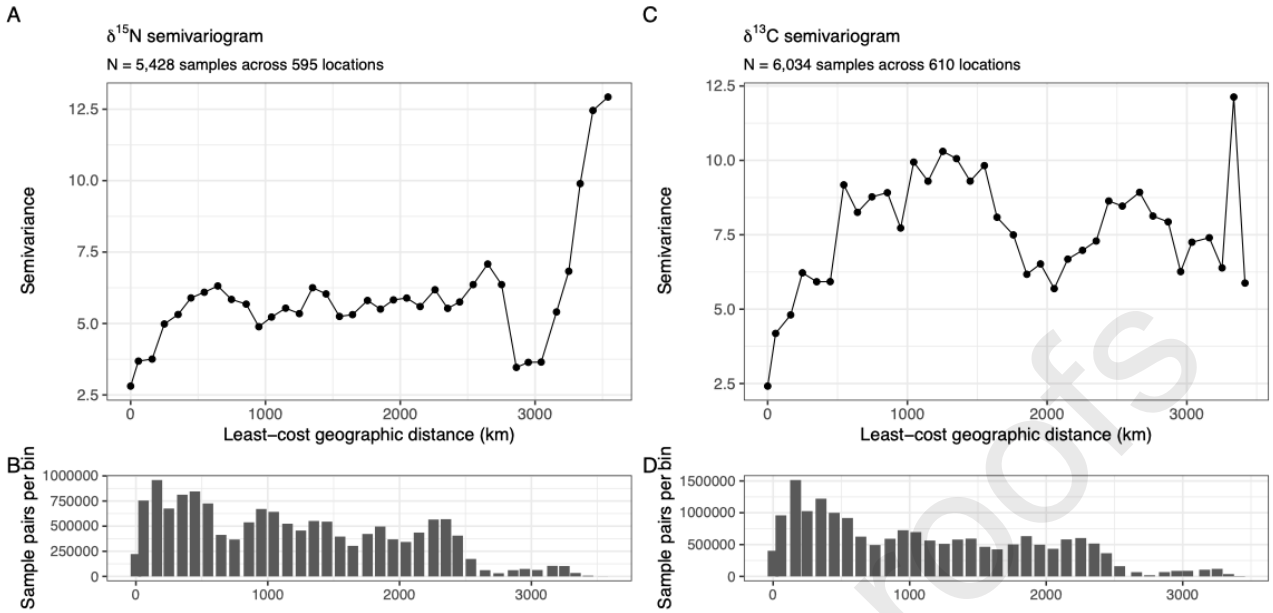

Figure 2. Sample semivariograms of $\delta^{15}N$ (A) and (B) $\delta^{13}C$ reference data computed using least-cost geographic distance across the Mediterranean Sea. Panels C and D show the number of sample pairs per distance bin; support declines substantially beyond ca. 2500 km.

3.4 INLA models

3.4.1 Model comparison

Comparisons of spatial vs non-spatial models showed that including a spatial field substantially improved both model fit (WAIC) and predictive accuracy (ρ) for $\delta^{15}N$ and $\delta^{13}C$. For $\delta^{15}N$ null models, WAIC decreased from 23,453.29 in the non-spatial model (M0) to 21,945.75 in its spatial counterpart (M0.SF), while ρ increased from 0.43 to 0.66. For $\delta^{13}C$, WAIC decreased from 26,490.21 (M0) to 24,215.33 (M0.SF), with ρ increasing from 0.59 to 0.79 (Table 2). Similar improvements were observed when comparing non-spatial covariate-based models (M1lin, M1sm) with their spatial counterparts (M1lin.SF, M1sm.SF; Table 2).

Within the spatial model set, the inclusion of environmental covariates improved model fit for $\delta^{15}N$ relative to the null spatial model when included as smooth terms, but not as linear fixed effects. For $\delta^{13}C$, the inclusion of covariates – either as linear or smooth terms – did not improve model fit relative to the null spatial model. For $\delta^{15}N$, the lowest WAIC values were obtained for the smooth covariate model (M1sm.SF: 21,873.78), compared to 21,945.75 for the null spatial model (M0.SF) and 21,948.82 for the linear covariate model (M1lin.SF). In contrast, for $\delta^{13}C$ the lowest WAIC values were obtained for the null spatial model (M0.SF: 24,215.33), with higher values for models including covariates (M1lin.SF: 24,257.29; M1sm.SF: 24,264.02). Based on WAIC, the best-performing models were therefore M1sm.SF for $\delta^{15}N$ and M0.SF for $\delta^{13}C$. Predictive accuracy, however, remained nearly unchanged across models ($\delta^{15}N$: ρ = 0.66-0.67; $\delta^{13}C$: ρ = 0.79; Table 2), indicating that improvements in WAIC were not accompanied by gains in predictive performance. Thus, while smooth covariate terms improved model fit for $\delta^{15}N$, they did not enhance predictive accuracy despite increased model complexity. Consistent with this, smooth covariate effects were weak and poorly constrained, with no clear or consistent trends (Fig. S.9).

Table 2. Model comparison results for the $\delta^{15}N$ and $\delta^{13}C$ models. Models tested the inclusion of a spatial field as a random effect and environmental covariates as either linear fixed effects or smooth terms. All models included category as a non-spatial random effect. Model fit was evaluated using the Watanabe-Akaike Information Criteria (WAIC), and predictive accuracy was assessed from the Pearson correlation coefficient (ρ) between observed and fitted values. The effective number of parameters (Eff. n parms) and most influential covariates (i.e., significant linear fixed effects or smooth terms with the largest attributed variance) are also reported. For correlations, the t, ρ, 95% confidence interval, and degrees of freedom (df) are shown. All correlations were statistically significant (p-value <0.001). Models are listed in order of increasing WAIC for each isotope, with ΔWAIC reported relative to the best model.

Model notation: M0 = null model (no environmental covariates); M1lin = model with linear covariates; M1sm = model with smooth covariates; ".SF" indicates inclusion of a spatial field.

Model	Model formula	WAIC	ΔWAIC	Eff. n parms	t	ρ	95% confidence interval	df	Significant covariates
$\delta^{15}N$									
M1sm.SF	Smooth + f(Category) + SF	21,873.78	na	251.73	66.04	0.67	0.65-0.68	5,426	Bathy, DIC, MLD, PC1
M0.SF	f(Category) + SF	21,945.75	71.97	245.63	64.90	0.66	0.65-0.68	5,426	na
M1lin.SF	Linear + f(Category) + SF	21,948.82	75.04	247.40	64.90	0.66	0.65-0.68	5,426	MLD
M1sm	Smooth + f(Category)	22,895.48	1,021.70	42.25	45.08	0.52	0.50-0.54	5,426	All
M1lin	Linear + f(Category)	23,346.84	1,473.06	14.19	36.93	0.45	0.43-0.47	5,426	Bathy, BT, MLD, PC1
M0	f(Category)	23,453.29	1,579.51	9.63	34.93	0.43	0.41-0.45	5,426	na
$\delta^{13}C$									

M0.SF	f(Category) + SF	24,215.33	na	464.18	99.31	0.79	0.78-0.80	6,032	na
M1lin.SF	Linear + f(Category) + SF	24,257.29	41.96	507.26	99.83	0.79	0.78-0.80	6,032	Bathy, MLD
M1sm.SF	Smooth + f(Category) + SF	24,264.02	48.69	575.72	101.56	0.79	0.78-0.80	6,032	Bathy, DIC, MLD, PC1
M1sm	Smooth + f(Category)	25,717.11	1,501.78	45.76	67.88	0.66	0.64-0.67	6,032	All
M1lin	Linear + f(Category)	26,220.12	2,004.79	17.53	60.57	0.61	0.60-0.63	6,032	Bathy, BT, DIC, PC1
M0	f(Category)	26,490.21	2,274.88	12.27	56.87	0.59	0.57-0.61	6,032	na

3.4.2 Spatial field random effect

Estimated spatial fields were characterized by short ranges and high variances across models (Fig. 3 and S.10), indicating that spatial isotope variability in the dataset non-attributable to environmental covariates (when present in the models) was dominated by strong small-scale structure. For $\delta^{15}N$, the smooth covariate model (M1sm.SF) yielded a mean spatial field range of 65.4 km (95% credible interval: 48.4-85.8 km). Similar ranges were obtained for the null spatial model (M0.SF: 75.5 km; 57.8-99.1 km) and the linear covariate model (M1lin.SF: 72.7 km; 54.4-96.7 km; Fig. 3A). Thus, including covariates resulted in only a marginal reduction in spatial range relative to the null model when modeled as smooth terms, and no reduction when modeled as linear effects. For $\delta^{13}C$, spatial field ranges were even shorter and similarly unaffected by the inclusion of covariates: M0.SF: 38.3 km (29.0-50.8 km), M1lin.SF: 32.4 km (23.6-44.2 km), and M1sm.SF: 33.6 km (24.2-46.2 km; Fig. 3B). Mean spatial ranges were only slightly greater than half of the maximum mesh edge length (100 km) for $\delta^{15}N$, and less than half for $\delta^{13}C$. For reference, the mean nearest-neighbor distance among unique sample locations was 22.2 ± 28.1 km (median 13.2 km) for $\delta^{15}N$ and 19.0 ± 38.7 km (median 7.0 km) for $\delta^{13}C$.

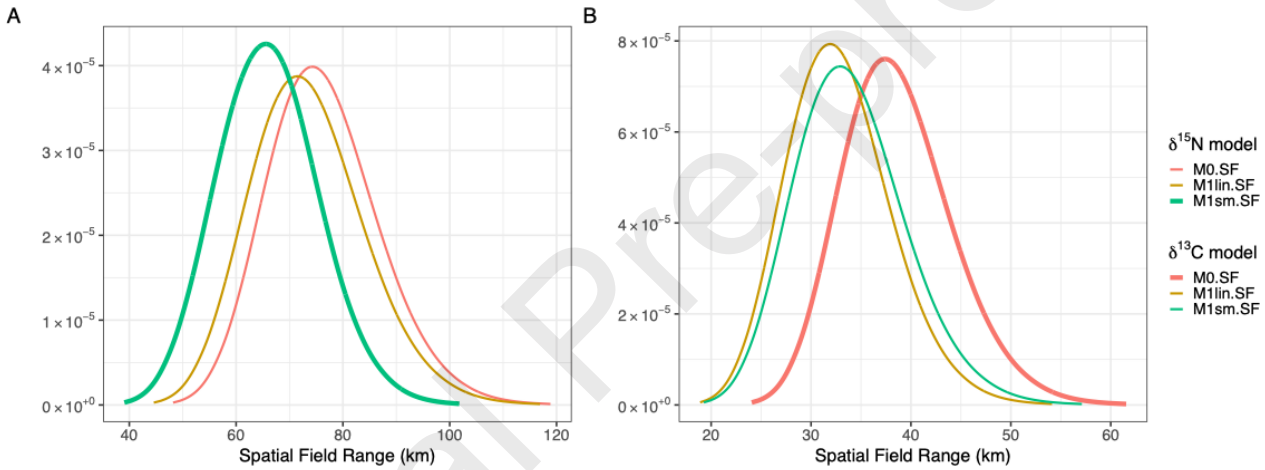

Figure 3. Posterior probability distributions of the spatial field range parameter for $\delta^{15}N$ (A) and $\delta^{13}C$ (B) models. All models include the spatial field and category as random effects. Models shown are: (i) null spatial models without covariates (M0.SF), ii) models with covariates as linear fixed effects (M1lin.SF), and iii) models with covariates as smooth terms (M1sm.SF). Thicker lines indicate the best-performing models based on WAIC (M1sm.SF for $\delta^{15}N$ and M0.SF for $\delta^{13}C$).

3.4.3 Non-spatial random effects

Marginal posterior distributions of the category random effect are shown in Fig. 4. Substantial isotopic variability among categories (ca. 4‰ for both $\delta^{15}N$ and $\delta^{13}C$) persisted across models, indicating this variation was largely independent of environmental covariates and continuous spatial structure. For $\delta^{15}N$, pico-nanoplankton had the lowest values, phytoplankton and suprabenthos the highest, and POM, sediment, and zooplankton were intermediate (Fig. 4A). For $\delta^{13}C$, POM, pico-nanoplankton and sediment showed the lowest values, followed by phytoplankton and zooplankton, with suprabenthos highest (Fig. 4B). Posterior distributions overlapped more for $\delta^{15}N$ than for $\delta^{13}C$. For $\delta^{15}N$, strong overlap occurred among POM, sediment, and zooplankton, and between phytoplankton and suprabenthos. In contrast, $\delta^{13}C$ posteriors showed clearer separation, with overlap mainly among POM, sediment, and pico-nanoplankton, and between phytoplankton and zooplankton, while suprabenthos remained distinct (Fig. 4).

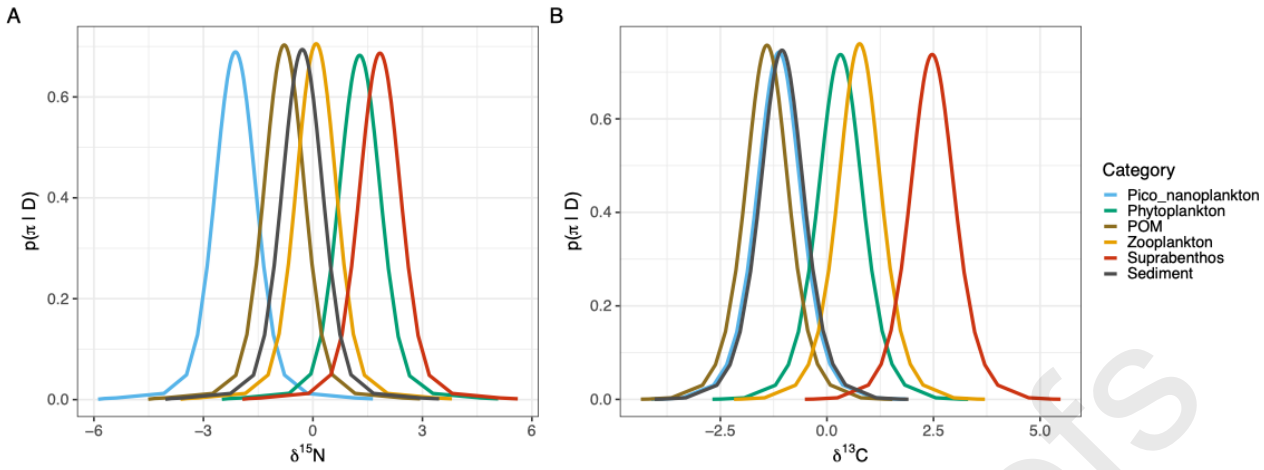

Figure 4. Marginal posterior distributions of the category random effect for $\delta^{15}N$ (A) and $\delta^{13}C$ (B) models. Each distribution ($\pi \mid D$) represents the probability density of the deviation of a given category from the overall mean isotope value, conditional on the data. Distributions are derived from the best-performing models (M1sm.SF for $\delta^{15}N$ and M0.SF for $\delta^{13}C$).

The inclusion of season as an additional random effect, using a reduced dataset (88-89% of samples for $\delta^{15}N$ and $\delta^{13}C$) with complete seasonal metadata, marginally improved WAIC values for both isotopes ($\delta^{15}N$: WAIC: Category + Season = 19,092.34 vs Category = 19,189.84; $\delta^{13}C$: WAIC: Category + Season = 21,129.12 vs Category = 21,167.19). However, predictive accuracy and spatial range remained unchanged (Table S.5). Posterior variability among seasons was substantially smaller (ca. 1‰ for $\delta^{15}N$, 0.5‰ for $\delta^{13}C$) than among categories, and seasonal posteriors overlapped extensively (Fig. S.12), with limited influence on category estimates.

3.4.4 Predicted isoscapes

Isoscapes predicted using the best-performing models (M1sm.SF for $\delta^{15}N$ and M0.SF for $\delta^{13}C$) showed that predictions were spatially constrained around areas with high sampling density (Fig. 5). In regions farther from sampled locations, predicted values rapidly reverted to the model's global mean: 4.1 ± 0.8‰ (mean ± SD) for $\delta^{15}N$ (Fig. 5A) and -22.5 ± 0.6‰ for $\delta^{13}C$ (Fig. 5B). Prediction uncertainty was high across the domain, with mean ± SD predicted variances of 1.5 ± 0.6‰ for $\delta^{15}N$ (range: 0.5-7.1‰) and 1.6 ± 0.9‰ for $\delta^{13}C$ (range: 0.4-7.8‰). The spatial distribution of uncertainty closely mirrored that of the predicted means, with lowest uncertainty at sampled locations and consistently high uncertainty across unsampled areas (Fig. 5C, D).

In both isoscapes, mean spatial variation in predicted values (0.8‰ for $\delta^{15}N$ and 0.6‰ for $\delta^{13}C$) was smaller than mean posterior uncertainty (1.5‰ and 1.6‰, respectively), indicating that spatial differences were weak relative to model uncertainty. The $\delta^{15}N$ isoscape showed apparent differences among discrete, well-sampled regions – for example, lower predicted values in the Gulf of Lion and Aegean Sea compared to higher values in the Balearic and Adriatic regions (Fig. 5A). These differences exceeded local prediction uncertainty within well-sampled regions, but did not persist across the distances separating those regions, such that spatial differences were not maintained across poorly sampled areas.

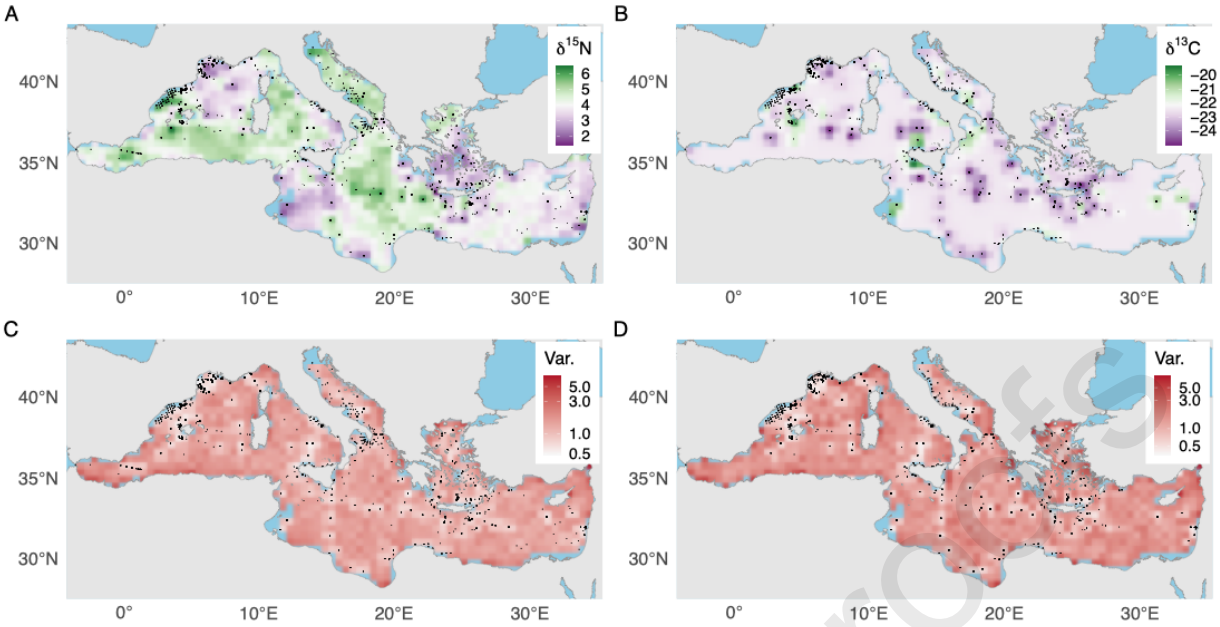

Figure 5. Predicted isoscape surfaces for $\delta^{15}N$ (A, C) and $\delta^{13}C$ (B, D) across the Mediterranean Sea. Panels show posterior means (A, B) and posterior variances (C, D) predicted by the best-performing models (M1sm.SF for $\delta^{15}N$ and M0.SF for $\delta^{13}C$). Variances are displayed on a $\log_{10}$ color scale for visualization. Points indicate sampling locations. Predictions represent geographic baseline isoscapes derived from six sample categories representing low-trophic-level food web compartments primarily supported by epipelagic production. Category was included as a non-spatial random effect to account for systematic differences among groups.

Predictions from models including covariates showed greater apparent structure than those from null spatial models (Fig. S.13-S.15). However, this structure primarily reflected the spatial distribution of the covariates used for prediction rather than improved recovery of isotope gradients. Relative to null models, predictive accuracy remained unchanged, spatial ranges did not decrease, and uncertainty remained high across the domain. Overall, covariate-based models did not produce more accurate or more spatially resolved predictions than the null spatial models.

4 Discussion

This study represents a first attempt to construct basin-scale isoscapes for the Mediterranean Sea using a large, opportunistically compiled dataset of $\delta^{15}N$ and $\delta^{13}C$ values from low-trophic-level compartments. Using a Bayesian INLA framework [24], we evaluated whether environmental covariates and spatial autocorrelation could resolve broad-scale (hundreds of kilometers) geographic structure in baseline isotope values while accounting for sample heterogeneity through a category random effect.

Our main finding is that spatial variance in the dataset was dominated by small-scale structure for both isotopes (ca. 40 km for $\delta^{13}C$ and 65 km for $\delta^{15}N$; Fig. 3), while the inclusion of environmental covariates did not improve predictive performance (Table 2). This contrasts with expectations for systems structured by broad-scale, environmental gradients, where covariates explain large-scale variation and the spatial field captures only weak, localized variance that cannot be attributed to the covariates or other nominally non-spatial random effects. Instead, both null and covariate-based models consistently produced short-range, high-variance spatial fields, indicating that the spatial

component primarily fitted strong, localized non-attributable variance, rather than coherent, basin-scale structure.

This pattern reflects a mismatch between the spatial structure of isotopic variation and the sampling design. While isotopic variation is expected to follow environmental gradients, the compiled dataset is not structured to resolve these gradients or to separate spatial from non-spatial sources of variation. Sampling is uneven relative to expected spatial variation, and non-spatial sources of variability (e.g., category, season, year, depth, taxonomy, method) are not only heterogeneous but also spatially clustered. As a result, non-spatial effects become confounded with space, and the spatial field absorbs variability arising from true fine-scale heterogeneity and unresolved, spatially structured non-spatial variation. This explains why spatial models outperformed non-spatial ones (Table 2) despite failing to resolve broad-scale gradients.

Consequently, predicted isoscapes are constrained to short distances and revert to near-uniform mean values outside well-sampled areas, limiting their ability to represent continuous basin-scale patterns. That is, predicted isoscapes primarily reflect the structure of the underlying dataset rather than spatially resolved isotopic baselines. Apparent regional differences – such as lower $\delta^{15}N$ values in the Gulf of Lion, Liguro-Provençal basin, and southeastern Mediterranean, and higher values in the Catalan-Balearic, Adriatic, and northern Aegean regions – likely reflect real contrasts among discrete, well-sampled regions. However, these differences cannot be reliably extrapolated beyond sampled areas. They are captured as localized features rather than components of a continuous spatial gradient, and their broader spatial extent and connectivity across poorly sampled regions remain unresolved.

4.1 Are there continuous isotopic gradients in the Mediterranean Sea?

Our results indicate that isotopic variation in the compiled dataset in both $\delta^{15}N$ and $\delta^{13}C$ is dominated by localized structure rather than clear basin-scale gradients. This pattern could arise from two non-mutually exclusive scenarios: broad-scale isotope gradients may be genuinely weak or absent in the Mediterranean Sea, or they exist but are not resolved given the characteristics of the compiled dataset.

Regarding the first scenario, several independent lines of evidence suggest that broad-scale isotope gradients *do* exist in the Mediterranean Sea. Key environmental drivers of $\delta^{13}C$ and $\delta^{15}N$ – temperature, nutrient availability, productivity, and nitrogen sources – differ markedly between the cooler, more eutrophic western basin and the warmer, oligotrophic eastern basin (Fig. 1 and S.5; [50, 133–136]). These variables underpin mechanistic isoscape models at global scales [3, 19, 21] and are established predictors in sample-based isoscapes (e.g., [24, 27]). The pronounced longitudinal gradients in these variables provide a strong theoretical basis for expecting corresponding isotope gradients in organic production. Empirical observations further support this expectation. Basin-scale variation in $\delta^{13}C$ DIC has been documented (<0.5‰; [159, 160]), consistent with productivity and temperature gradients. Regional differences in $\delta^{13}C$ and/or $\delta^{15}N$ values have also been reported across a range of taxa and ecosystem compartments, including POM [40], crustaceans [161], cephalopods [162], fishes [163], and sea turtle hatchlings [164], as well as at finer spatial scales in coastal fishes [165, 166]. Even within our dataset, winter POM samples show consistent, albeit subtle, differences between the western and eastern basins ($\delta^{15}N$: 0.4‰, W = 46206, p-value <0.05; $\delta^{13}C$: 1.2‰, W = 41350, p-value <0.05). Similarly, the full $\delta^{15}N$ dataset (and corresponding isoscape) supports differences among discrete, well-sampled regions, although spatial modeling cannot determine whether these represent continuous gradients or isolated regional signals (Fig. 5). Taken together, these observations indicate that isotopic gradients likely exist at both basin and regional scales in the Mediterranean Sea.

Nonetheless, basin-scale gradients may be relatively weak. For carbon, the longitudinal temperature gradient is modest (ca. 5 °C across the basin; Fig. 1 and S.5) compared to the stronger latitudinal contrasts (2-3-fold larger) that drive pronounced $\delta^{13}C$ isoscapes in larger oceanic systems [25, 26], though comparable to variation in UK shelf seas [24]. Similarly, chlorophyll *a* concentrations in the Mediterranean (ca. 0.2 mg m^{-3}; Fig. 1 and S.5) are substantially lower (ca. 1-2 orders of magnitude) than in more productive systems [24, 25, 27, 107], potentially resulting in weaker isotope gradients. Moreover, environmental controls can act in opposing directions – for example, cooler temperatures in the west tend to lower phytoplankton $\delta^{13}C$ values [137], whereas higher nutrient availability can elevate it through increased growth rates [138–141]. For nitrogen, contrasts in source contributions between the two basins [65, 66, 147] may be dampened by overlapping processes [69, 143–145, 167, 168], including N_2 fixation in both basins [169–171] and variable anthropogenic inputs. Basin-scale circulation and mixing further homogenize surface baselines, reducing the isotopic expression of underlying biogeochemical gradients (e.g., [40, 90]). Interannual variability in circulation and Atlantic inflow may additionally disrupt or weaken persistent large-scale patterns [172].

4.2 Dataset limitations and implications for modeling continuous isotopic gradients

While environmental gradients and biogeochemical processes may constrain the strength of isotope patterns, the ability to detect such gradients ultimately depends on how the data are structured relative to those processes. In this study, the compiled dataset was not suitably structured to resolve spatial isotopic variation expected along environmental gradients. Sampling was uneven in space and confounded multiple sources of variability (e.g., category, season, year, depth, taxonomy, method), which were not independently represented across the basin and were, to varying extents, themselves spatially structured. Although hierarchical models are designed to accommodate unbalanced sampling, the co-occurrence of these sources of variability in space limits the ability to separate spatial from non-spatial effects. As a result, spatial and non-spatial sources of variation could not be effectively disentangled.

The key limitation is not simply uneven sampling, but that non-spatial sources of variation are themselves spatially structured. When non-spatial factors are spatially clustered or covary with environmental gradients, they become confounded with space. Under these conditions, non-spatial variability can be expressed as spatial signal, and the spatial field absorbs variance arising from both true geographic structure and unresolved, spatially structured non-spatial effects. Consequently, the spatial component does not represent purely geographic variation, but reflects the combined structure of the data.

The issue is further amplified by the spatial distribution of sampling. Observations are strongly concentrated in coastal environments, while offshore regions – particularly in the southern and eastern Mediterranean – are comparatively underrepresented. Coastal environments are inherently more isotopically variable due to localized biogeochemical inputs (e.g., river plumes, lagoons), short-term temporal fluctuations, complex trophic interactions, and anthropogenic influences (e.g., [31, 68, 83, 98, 173–175]), reducing signal-to-noise ratios in the data. In contrast, offshore regions typically exhibit lower variability and provide the spatial context necessary to resolve basin-scale gradients. This imbalance does not simply reduce coverage, but disproportionately weights model fitting toward highly variable, spatially clustered observations, further increasing the likelihood that non-spatial variability is expressed as spatial structure.

Among non-spatial effects, sample category was the only factor that could be consistently modeled across the full dataset, yet it captured only part of the variability, accounting for ca. 32.8-38.5% (for $\delta^{15}N$ and $\delta^{13}C$, respectively) of the combined category and residual variance. Substantial differences

among categories (ca. 4‰ for both $\delta^{15}N$ and $\delta^{13}C$) persisted across models, confirming that category represents an important source of isotopic variation independent of environmental covariates and spatial structure. If unaccounted for, such variability could bias inference, as differences of this magnitude represent a major portion of the spatial variance typically observed in marine isoscapes. While the category random effect captured some structured differences among groups, posterior distributions often overlapped between ecologically distinct categories or deviated from expected trophic patterns (Fig. 4), particularly for $\delta^{15}N$, which is typically trophically structured due to substantial trophic discrimination [176–178]. For instance, zooplankton, as consumers, would be expected to exhibit higher $\delta^{15}N$ than phytoplankton, yet the reverse was observed (Fig. 4A). These inconsistencies likely arise because category distributions covary with location and other unmodeled factors, rather than reflecting purely ecological differences. Consequently, the category effect absorbed both true group-level differences and spatially confounded or non-categorical variability, limiting its interpretability.

Other key sources of variation – particularly season and depth - were likely among the strongest drivers of isotopic variability (e.g., [36, 38, 102, 103, 173, 179, 180]) but could not be reliably incorporated due to incomplete or inconsistent metadata and their uneven, spatially structured representation. For instance, sampling season was often missing or not comparable across regions with differing climatic and oceanographic regimes (e.g., eastern and western basins) and among sample types with different isotopic incorporation rates (e.g., phytoplankton vs suprabenthic invertebrates). Critically, season and depth were not sufficiently represented across space and categories to support their inclusion as random effects in the full dataset. Including season as an additional crossed random effect in a reduced dataset with complete metadata marginally improved model fit but did not enhance predictive performance or alter spatial predictions (Table S.5), indicating that additional model complexity described internal dataset structure rather than resolving underlying processes. Under these conditions, season likely functions in part as a sampling block (e.g., reflecting individual surveys or cruises) rather than representing a coherent temporal signal, as also suggested by the lack of consistent patterns in posterior distributions (Fig. S.12). Similarly, depth-related processes – including subsurface production, vertical transport, and remineralization – introduce additional variability, as reworking extends trophic pathways before incorporation into sampled pools (e.g., POM), thereby modifying $\delta^{15}N$ and $\delta^{13}C$ values relative to surface producers [35, 39, 40, 181]. Such variability cannot be separated from surface signals under the available sampling design. Limited vertical resolution further constrains the ability to resolve these effects, which would likely require fully three-dimensional modeling approaches.

We argue that, taken together, these factors result in a low signal-to-noise ratio, in which spatially structured variation is obscured by unresolved local and non-spatial variability. The short spatial ranges and weak predictive performance observed across models therefore reflect the interaction between structured sources of variation and a sampling design that is not aligned with them, rather than the absence of isotopic gradients in the system.

Importantly, these limitations do not reflect poor data quality. The compiled dataset integrates high-quality observations from numerous studies (Table S.1) and is large relative to many existing marine isoscapes (>6000 samples from >600 sites), comparable to or exceeding that of datasets used in isoscapes for the Southern Ocean (N >3000 samples [26]), North Atlantic (N = 570 [27]), or UK shelf seas (N = 627 [24]). Metadata incompleteness or inconsistency should not be interpreted as a deficiency: in studies not designed for spatial analysis, such information is often unnecessary. Similar gaps are widespread – for example, Skinner et al. [182] reported that 17% of isotope studies in coral reef ecosystems lacked sufficient detail to identify sampling time or location. Rather the limitation lies in the lack of alignment between sampling design and the requirements of spatial modeling. There

is clear structure in the data – and thus potential to generate informative isoscapes – but the opportunistic nature of sampling prevents meaningful separation of spatial and non-spatial components of isotopic variation.

More broadly, this case illustrates a general limitation of applying variance-partitioning spatial models to opportunistically compiled datasets. Isoscapes can be derived when sampling designs allow key sources of variation to be represented across space in a way that enables their effects to be distinguished statistically. When this condition is not met, variance is partitioned according to the structure of the data rather than underlying processes, and resulting isoscapes cannot be interpreted as true geographic signals. These challenges are not unique to the Mediterranean, but are likely to arise in any system where sampling is unstructured relative to spatially and ecologically structured sources of variation. For spatial isotope applications, reference datasets must be built from spatially explicit, coordinated, and appropriately replicated sampling efforts – such as basin-scale epipelagic surveys or Continuous Plankton Recorder-type programs [183]. High-quality data alone are not sufficient; alignment between sampling structure and modeling requirements is essential.

4.3 Implications for spatial inference from compiled datasets and future sampling design

Broad-scale gradients in $\delta^{15}N$ and $\delta^{13}C$ values have been successfully identified in several marine systems using opportunistic or mixed-source datasets (e.g., [22, 25–27]. However, these cases were generally more amenable to spatial modeling than the Mediterranean Sea. Samples were typically more homogenous and often restricted to specific epipelagic compartments (e.g., POM [26]; copepods [25, 27] or gelatinous plankton [24]), and in some cases were explicitly collected for isoscape construction [24]. This allowed models to more effectively separate spatial structure from species- or time-related effects and recover coherent isotope patterns. In contrast, the Mediterranean dataset integrates a broader range of sample types across an environmentally complex and dynamic basin. While this increases ecological relevance and spatial coverage, it also introduces multiple, interacting sources of variability that limit the ability of spatial models to accurately partition variance.

These findings have broader implications as compiled isotope datasets become increasingly available (e.g., [46–48]; see also [45, 184]) and are applied to spatial modeling [185]. When key sources of variance are uncontrolled or spatially confounded, even advanced Bayesian spatial models cannot compensate for limitations in sampling design. This has consequences not only for isoscape construction but for any analysis relying on hierarchical or spatial inference from opportunistic data.

Several diagnostic indicators can help assess whether a dataset is suitable for spatial applications: (i) semivariograms showing only short-range autocorrelation; (ii) spatial fields with short estimated ranges and high variances; (iii) random effects (e.g., category) with posterior distributions that deviate from ecological expectations; and (iv) environmental covariates that fail to improve predictive performance or to reduce the spatial field's range and variance. Together, these signals indicate that spatial isotope structure is unresolved. In such cases, isoscape predictions should not be extrapolated beyond sampled locations, and even local predictions should be interpreted cautiously, as the spatial field may primarily reflect non-attributable variance rather than genuine local signals. More broadly, these limitations extend beyond spatial analyses. In non-spatial analyses (e.g., mixing models, niche analyses, or time-series), it may be even more difficult to determine whether a lack of predictable structure reflects true ecological variability or an artefact from uncontrolled variance in opportunistic datasets.

To support robust spatial inference, sampling design must be aligned with the structure of isotopic variation. This does not require uniform coverage, but key sources of variability must be represented across space in a way that allows their effects to be distinguished statistically. In practice, this means ensuring that different levels of important factors (e.g., category, season, depth, etc.) are not systematically clustered in specific regions or confounded with spatial gradients.

Future efforts in the Mediterranean and similar systems should prioritize systematic, targeted, and coordinated sampling strategies. To separate spatial from non-spatial effects, key sources of variance should be represented across space at scales comparable to observed or expected autocorrelation ranges. Replication does not need to occur at every location, but variation must be structured such that contrasts can be estimated independently of location. Stratified designs (e.g., inshore vs offshore systems; see [120, 186]) may also be effective when environmental drivers operate at different scales. Without such structure, increasing sample size alone will not improve inference, as unresolved variability will continue to be absorbed into spatial components. In contrast, fine-scale, structured sampling – particularly in spatially heterogeneous areas such as coastal and island systems – would allow non-spatial variance to be explicitly modeled, reduce overfitting by the spatial field, and improve the detection of meaningful gradients. That said, resolving spatial variation across multiple scales simultaneously remains logistically constrained: capturing kilometer-scale variability across the entire Mediterranean would require sampling densities that are not realistically achievable. Where full standardization is not feasible, comprehensive, high-quality metadata remain essential to ensure that data structure can be incorporated into models.

Large-scale coordinated programs such as GEOTRACES [187] demonstrate the feasibility of spatially extensive, intercalibrated sampling. In the Mediterranean, similar progress could be achieved by integrating isotope analyses into existing monitoring programs (e.g., MEDITS [188] MEDIAS [189], PELMED [190]). Embedding isotope sampling within ongoing surveys would also align with ecosystem-based monitoring frameworks [191]. Adding $\delta^{13}C$ and $\delta^{15}N$ analyses to routine sampling of low-mid trophic level organisms – such as benthic filter feeders (e.g., bivalves [28, 122, 149]) and pelagic species (e.g., forage fish, scyphomedusae [24]) – would provide spatially coherent proxies for baseline variation at relatively low cost, complementing efforts under Descriptor 4 ("Marine Food Webs") of the EC Marine Strategy Framework Directive (MSFD; [192]**)** to assess trophic structure. Such taxa offer advantages for isoscape development: primary producers and POM are often too dynamic to resolve large-scale patterns, zooplankton often include mixed trophic strategies, and higher trophic levels integrate signals over too broad spatial and temporal scales. In contrast, shorter-lived forage fish and similar organisms provide a balance between spatial coverage, ecological integration, and limited mobility [193, 194].

Ultimately, progress toward reliable isoscapes in the Mediterranean region and elsewhere will depend not on data volume alone, but alignment between sampling strategies and modeling objectives.

5 Conclusions

We compiled thousands of stable isotope measurements from across the Mediterranean Sea, revealing substantial isotopic variation and spatial structuring at multiple ecological and spatial scales across the region. These patterns indicate that meaningful isotopic heterogeneity exists within Mediterranean food web baselines and confirm that isotopic variation in the basin contains a spatially informative signal. However, advanced Bayesian models were unable to reliably resolve this heterogeneity into a single continuous isoscape from the available opportunistic dataset, despite its size and the high quality of the individual studies. This does not imply isotopic homogeneity or the absence of spatial gradients across the Mediterranean, but rather an inability to resolve and reliably generalize those

gradients given the mismatch between sampling design and the requirements of spatial inference. Our results demonstrate that even sophisticated hierarchical models do not yield reliable isoscapes when sampling is not structured relative to the underlying spatial and ecological gradients [193].

The compiled dataset nevertheless represents a valuable resource and diagnostic framework. Beyond documenting basin-wide isotopic variability, it provides empirical insight into the conditions under which spatial inference succeeds or fails, and therefore informs future sampling strategies. Assembled from thousands of measurements spanning the Mediterranean basin, it represents one of the most comprehensive stable isotope syntheses currently available for the region. Reliable isoscape development will require systematic, spatially explicit, and targeted sampling designs integrated with coordinated monitoring programs to constrain key sources of variability. In the Mediterranean, this challenge is amplified by oceanographic and ecological features that promote strong fine-scale variability, including oligotrophy, restricted circulation, localized inputs, mesoscale processes such as fronts, eddies, and upwelling, and complex habitat mosaics [98, 102, 129, 195, 196], representing an ecological limit to the generalization of isotopic baselines. More broadly, as large datasets become increasingly available, caution is warranted (see [197]). Opportunistic datasets are often biased [24, 26, 27, 198], and sophisticated hierarchical models are no substitute for well-structured sampling. Robust ecological inference therefore depends not only on data availability, but on critically evaluating dataset structure and aligning sampling design with analytical objectives.

CRediT authorship contribution statement

Sarah Magozzi: Conceptualization, Data curation, Formal analysis, Investigation, Methodology, Supervision, Visualization, Writing – original draft, Writing – review and editing. Clive N. Trueman: Conceptualization, Investigation, Methodology, Supervision, Visualization, Writing – original draft, Writing – review and editing. Matthew R. D. Cobain: Formal analysis, Investigation, Methodology, Visualization, Writing – original draft, Writing – review and editing. Kirsteen M. MacKenzie, Katie St. John Glew, José A. Canseco, Eric Díaz-Delgado, Emanuela Fanelli, Paola Rumolo, Joan E. Cartes, Boris Espinasse: Data curation, Investigation, Visualization, Writing – review and editing. Davide Agnetta, Marta Albo-Puigserver, Carmen Alomar, Francesca Alvisi, Fabio Badalamenti, Daniela Bănaru, Daniela Berto, Angelo Bonanno, Chiara Bonaviri, Lucia Bongiorni, Yeşim Büyükateş, Antonio Miguel Calafat Frau, Elisa Camatti, Carolina Cantoni, Luis Cardona, Antoine Carlier, Michela Castellano, Jacopo Chiggiato, Tamara Cibic, Ilaria Conese, Martina Coppari, David Costalago, Pierre Cresson, Isabella D'Ambra, Kirstin Dähnke, Audrey M. Darnaude, Salud Deudero, Daria Ezgeta-Balić, Michele Giani, Alexandra Gogou, Gérald Grégori, Tamar Guy-Haim, Mireille L. Harmelin-Vivien, Simon Jennings, Aristomenis P. Karageorgis, Rolf Koppelmann, Nikolaos Lampadariou, Leonardo Langone, Camilla Liénart, Maria Grazia Mazzocchi, Antonio Mazzola, Travis B. Meador, Louise Merquiol, Marc Metzke, Stefano Miserocchi, Jürgen Möbius, Behzad Mostajir, Laure Mousseau, Joan Navarro, Nives Ogrinc, Marco Pansera, Silvio Pantoja-Gutiérrez, Vanesa Papiol, Constantine Parinos, Catalina Pasqual, Alexandra S. Pavlidou, Rut Pedrosa-Pàmies, John Pinnegar, Nicholas V. C. Polunin, Maria Protopapa, Daniel J. Repeta, Nadia Sabatino, Julian P. Sachs, Anna Sanchez-Vidal, Gianluca Sarà, Nicolas Savoye, Anna Schroeder, Ester Skylaki, Daniel M. Sigman, Geraldina Signa, Guy Sisma-Ventura, Ioanna Stavrakaki, Ulrich Struck, Javier A. Tesán-Onrubia, Tommaso Tesi, Sinan Uzundumlu, Maria Valls, Salvatrice Vizzini, Soultana Zervoudaki, Salem W. Zgozi, Annamaria Zoppini, Barbara Zorica: Data curation, Investigation, Writing – review and editing. Spyros Chaikalis, Pascal Conan: Data curation. Trevor J. Willis: Conceptualization, Funding acquisition, Investigation, Supervision, Visualization, Writing – review and editing.

Declaration of competing interest

The authors declare that they have no financial or personal relationships with individuals or organizations that could inappropriately influence or bias the work presented in this manuscript.

Acknowledgements

The authors thank Prof. Kay-Christian Emeis for contributing to dataset IDs 72 and 88 compiled in this study. Sarah Magozzi was supported by the Stazione Anthon Dohrn and the PNRR National Biodiversity Future Center to lead and perform this research. We acknowledge the funding sources that supported the generation of datasets included in this compilation: the "Severo Ochoa Centre of Excellence" accreditation (CEX2024-001494-S) to the ICM-CSIC; the Spanish-funded IDEA (CICYT) (ref. REN2002-04535-C01-02/MAR), BIOMARE (ref. CTM2006-13508-CO2-02/MAR: Identification of BIOmarkers of the anthropogenic impact on MARine communities: an Ecosystemic approach), and ANTROMARE (ref. CTM2009-12214-C02-01/MAR) projects; the French SOMLIT Network, part of the French Research Infrastructure ILICO, funded by the CNRS, French Marine Universities, and ILICO; dataset ID 89 was supported by the CONTAMPUMP project (ANR JCJC #19-CE34-0001-01), the MERITE-HIPPOCAMPE project and campaign funded through the cross-disciplinary "Pollution & Contaminants" axis of the CNRS-INSU MISTRALS program (joint action of the MERMEX-MERITE and CHARMEX subprograms), and by the IRD French-Tunisian International Joint Laboratory (LMI) COSYS-Med; dataset ID 93 benefited from the SOMLIT survey, and analysis costs were supported by the INSU/EC2CO project ZOO-INDEX (Call 2021; PIs: D. Bănaru & F. Carlotti) under the French National Program CNRS-INSU-EC2CO (Ecosphère Continentale et Côtière); the OCEAN-CERTAIN campaign was supported by the project OCEAN-CERTAIN (GA #603773) of the European Commission; Louise Merquiol's PhD fellowship funded by the Stazione Zoologica Anton Dohrn (Open University – Stazione Zoologica Anton Dohrn PhD Program); Nives Ogrinc's research supported by the Slovenian Research and Innovation Agency under the program P1-0143. Research by Salvatrice Vizzini, Antonio Mazzola, and Geraldina Signa was funded by the project INTERREG-MED BLUEISLANDS (Ref: 613/1MED15_3.1_M12_273). Research by Alexandra Gogou, Constantine Parinos, Aristomenis P. Karageorgis, Nikolaos Lampadariou, Alexandra S. Pavlidou, Spyros Chaikalis, Ester Skylaki, and Ioanna Stavrakaki was supported by the following projects: "Support for upgrading the operation of the National Network for Climate Change - CLIMPACT" (Grant Agreement: 2023NA11900001, MIS 5201588), funded by national Greek funds under the Ministry of Development & Investment; "MARine monitoring system of the Hellenic Seas using REmote sensing satellite data and insitu measurements - MARRE" project (T1EDK-02966) (EPAnEK, ESPA 2014–2020; European Regional Development Fund); "Integrated Observatories of the Greek Seas" (KRIPIS; NSRF/GR – EU ESPA 2007-2013); "Monitoring Program for the Implementation of the Marine Strategy Framework Directive (MSFD; 2008/56/EC) in the Hellenic Seas" (EPAnEK 2014-2020 GR / European Regional Development Fund); MarinERA (EU-RTD, FP6 ERA-NET), REDECO (CTM2008-04973-E/MAR), and MEDECOS (CTM2008-04365-E) projects; PERLE cruise funded in the framework of the French MISTRALS-MERMEX (CNRS/INSU) project: CONAN Pascal, DURRIEU DE MADRON Xavier (2019) PERLE2 cruise, RV Pourquoi pas?, https://doi.org/10.17600/18000865. Rut Pedrosa-Pàmies' research was supported by the EU-funded project PERSEUS (GA 287600), the Greek-co-funded project KRIPIS, and REDECO, BIOFUN (CTM2007-28739-E), and MEDECO projects; Yeşim Büyükateş' and Sinan Uzundumlu's research by Çanakkale Onsekiz Mart University Research Foundation (BAP, Project #FDK 2016/869). Daniel J Repeta was supported by NSF OCE-9711702, Daniel M Sigman by NSF OCE-9981479, and Silvio Pantoja-Gutiérrez by funds from the Johnson Foundation while at WHOI.

Data availability

All data and R code used in this study will be publicly archived on Zenodo upon acceptance. For peer-review purposes, these materials are available to reviewers through the private link provided during submission.

References

[1] Bowen GJ. Isoscapes: Spatial Pattern in Isotopic Biogeochemistry. *Annu Rev Earth Planet Sci* 2010; 38: 161–187. https://doi.org/10.1146/annurev-earth-040809-152429

[2] West JB, Bowen GJ, Dawson TE, et al. (eds). *Isoscapes: Understanding movement, pattern, and process on Earth through isotope mapping*. Springer Dordrecht, 2010. https://doi.org/10.1007/978-90-481-3354-3

[3] Schmittner A, Gruber N, Mix AC, et al. Biology and air–sea gas exchange controls on the distribution of carbon isotope ratios ($\delta^{13}C$) in the ocean. *Biogeosciences* 2013; 10: 5793–5816. https://doi.org/10.5194/bg-10-5793-2013

[4] Schmittner A, Somes CJ. Complementary constraints from carbon (^{13}C) and nitrogen (^{15}N) isotopes on the glacial ocean's soft-tissue biological pump. *Paleoceanography* 2016; 31: 669–693. https://doi.org/10.1002/2015PA002905

[5] Buchanan PJ, Chase Z, Matear RJ, et al. Marine nitrogen fixers mediate a low latitude pathway for atmospheric CO_2 drawdown. *Nat Commun* 2019; 10: 4611. https://doi.org/10.1038/s41467-019-12549-z

[6] Buchanan PJ, Tagliabue A, de la Vega C, et al. Oceanographic and biogeochemical drivers cause divergent trends in the nitrogen isoscape in a changing Arctic Ocean. *Ambio* 2022; 51: 383–397. https://doi.org/10.1007/s13280-021-01635-6

[7] Vander Zanden HB, Tucker AD, Hart KM, et al. Determining origin in a migratory marine vertebrate: a novel method to integrate stable isotopes and satellite tracking. *Ecological Applications* 2015; 25: 320–335. https://doi.org/10.1890/14-0581.1

[8] Trueman CN, MacKenzie KM, St John Glew K. Stable isotope-based location in a shelf sea setting: accuracy and precision are comparable to light-based location methods. *Methods Ecol Evol* 2017; 8: 232–240. https://doi.org/10.1111/2041-210X.12651

[9] St John Glew K, Wanless S, Harris MP, et al. Sympatric Atlantic puffins and razorbills show contrasting responses to adverse marine conditions during winter foraging within the North Sea. *Mov Ecol* 2019; 7: 33. https://doi.org/10.1186/s40462-019-0174-4

[10] Trueman CN, Jackson AL, Chadwick KS, et al. Combining simulation modeling and stable isotope analyses to reconstruct the last known movements of one of Nature's giants. *PeerJ* 2019; 7: e7912. https://doi.org/10.7717/peerj.7912

[11] Navarro J, Coll M, Somes CJ, et al. Trophic niche of squids: Insights from isotopic data in marine systems worldwide. *Deep Sea Research Part II: Topical Studies in Oceanography* 2013; 95: 93–102. https://doi.org/10.1016/j.dsr2.2013.01.031

[12] Jennings S, van der Molen J. Trophic levels of marine consumers from nitrogen stable isotope analysis: estimation and uncertainty. *ICES Journal of Marine Science* 2015; 72: 2289–2300. https://doi.org/10.1093/icesjms/fsv120

[13] Bird CS, Veríssimo A, Magozzi S, et al. A global perspective on the trophic geography of sharks. *Nat Ecol Evol* 2018; 2: 299–305. https://doi.org/10.1038/s41559-017-0432-z

[14] Pethybridge H, Choy CA, Logan JM, et al. A global meta-analysis of marine predator nitrogen stable isotopes: Relationships between trophic structure and environmental conditions. *Global Ecology and Biogeography* 2018; 27: 1043–1055. https://doi.org/10.1111/geb.12763

[15] Chesson LA, Valenzuela LO, O'Grady SP, et al. Links between Purchase Location and Stable Isotope Ratios of Bottled Water, Soda, and Beer in the United States. *J Agric Food Chem* 2010; 58: 7311–7316. https://doi.org/10.1021/jf1003539

[16] Slesser HW, Trueman CN. Traceability of the Norway Lobster *Nephrops norvegicus* in UK Shelf Seas: A Stable Isotope Approach. *J Shellfish Res* 2021; 40: 153–160. https://doi.org/10.2983/035.040.0115

[17] Cusa M, St John Glew K, Trueman C, et al. A future for seafood point-of-origin testing using DNA and stable isotope signatures. *Rev Fish Biol Fish* 2022; 32: 597–621. https://doi.org/10.1007/s11160-021-09680-w

[18] Martino JC, Trueman CN, Mazumder D, et al. The universal imprint of oxygen isotopes can track the origins of seafood. *Fish and Fisheries* 2022; 23: 1455–1468. https://doi.org/10.1111/faf.12703

[19] Magozzi S, Yool A, Vander Zanden HB, et al. Using ocean models to predict spatial and temporal variation in marine carbon isotopes. *Ecosphere* 2017; 8: e01763. https://doi.org/10.1002/ecs2.1763

[20] Trueman CN, St John Glew K. Isotopic Tracking of Marine Animal Movement. In: *Tracking Animal Migration with Stable Isotopes*. Elsevier, 2019, pp. 137–172. https://doi.org/10.1016/B978-0-12-814723-8.00006-4

[21] Somes CJ, Schmittner A, Galbraith ED, et al. Simulating the global distribution of nitrogen isotopes in the ocean. *Global Biogeochem Cycles* 2010; 24: GB4019. https://doi.org/10.1029/2009GB003767

[22] McMahon KW, Hamady LL, Thorrold SR. A review of ecogeochemistry approaches to estimating movements of marine animals. *Limnol Oceanogr* 2013; 58: 697–714. https://doi.org/10.4319/lo.2013.58.2.0697

[23] MacKenzie KM, Longmore C, Preece C, et al. Testing the long-term stability of marine isoscapes in shelf seas using jellyfish tissues. *Biogeochemistry* 2014; 121: 441–454. https://doi.org/10.1007/s10533-014-0011-1

[24] St John Glew K, Graham LJ, McGill RAR, et al. Spatial models of carbon, nitrogen and sulphur stable isotope distributions (isoscapes) across a shelf sea: An INLA approach. *Methods Ecol Evol* 2019; 10: 518–531. https://doi.org/10.1111/2041-210X.13138

[25] Espinasse B, Hunt BPV, Batten SD, et al. Defining isoscapes in the Northeast Pacific as an index of ocean productivity. *Global Ecology and Biogeography* 2020; 29: 246–261. https://doi.org/10.1111/geb.13022

[26] St John Glew K, Espinasse B, Hunt BPV, et al. Isoscape Models of the Southern Ocean: Predicting Spatial and Temporal Variability in Carbon and Nitrogen Isotope Compositions of Particulate Organic Matter. *Global Biogeochem Cycles*; 35: e2020GB006901. https://doi.org/10.1029/2020GB006901

[27] Espinasse B, Sturbois A, Basedow SL, et al. Temporal dynamics in zooplankton δ13C and δ15N isoscapes for the North Atlantic Ocean: Decadal cycles, seasonality, and implications for predator ecology. *Front Ecol Evol*; 10: 986082. https://doi.org/10.3389/fevo.2022.986082

[28] Jennings S, Warr KJ. Environmental correlates of large-scale spatial variation in the δ15N of marine animals. *Mar Biol* 2003; 142: 1131–1140. https://doi.org/10.1007/s00227-003-1020-0

[29] Radabaugh KR, Hollander DJ, Peebles EB. Seasonal $\delta^{13}C$ and $\delta^{15}N$ isoscapes of fish populations along a continental shelf trophic gradient. *Cont Shelf Res* 2013; 68: 112–122. https://doi.org/10.1016/j.csr.2013.08.010

[30] Schloesser RW, Rooker JR, Louchuoarn P, et al. Interdecadal variation in seawater $\delta^{13}C$ and $\delta^{18}O$ recorded in fish otoliths. *Limnol Oceanogr* 2009; 54: 1665–1668. https://doi.org/10.4319/lo.2009.54.5.1665

[31] Bănaru D, Carlotti F, Barani A, et al. Seasonal variation of stable isotope ratios of size-fractionated zooplankton in the Bay of Marseille (NW Mediterranean Sea). *J Plankton Res* 2014; 36: 145–156. https://doi.org/10.1093/plankt/fbt083

[32] Liénart C, Garbaras A, Qvarfordt S, et al. Spatio-temporal variation in stable isotope and elemental composition of key-species reflect environmental changes in the Baltic Sea. *Biogeochemistry* 2022; 157: 149–170. https://doi.org/10.1007/s10533-021-00865-w

[33] Giraldo C, Cresson P, MacKenzie K, et al. Insights into planktonic food-web dynamics through the lens of size and season. *Sci Rep* 2024; 14: 1684. https://doi.org/10.1038/s41598-024-52256-4

[34] Liénart C, Fournioux A, Garbaras A, et al. Bivalve tissues as a recorder of multidecadal global anthropogenic and climate-mediated change in coastal areas. *Limnol Oceanogr Lett* 2024; 9: 653–666. https://doi.org/10.1002/lol2.10399

[35] Saino T, Hattori A. ^{15}N natural abundance in oceanic suspended particulate matter. *Nature* 1980; 283: 752–754. https://doi.org/10.1038/283752a0

[36] Polunin NVC, Morales-Nin B, Pawsey WE, et al. Feeding relationships in Mediterranean bathyal assemblages elucidated by stable nitrogen and carbon isotope data. *Mar Ecol Prog Ser* 2001; 220: 13–23. https://doi.org/10.3354/meps220013

[37] Koppelmann R, Böttger-Schnack R, Möbius J, et al. Trophic relationships of zooplankton in the eastern Mediterranean based on stable isotope measurements. *J Plankton Res* 2009; 31: 669–686. https://doi.org/10.1093/plankt/fbp013

[38] Fanelli E, Papiol V, Cartes JE, et al. Trophic webs of deep-sea megafauna on mainland and insular slopes of the NW Mediterranean: a comparison by stable isotope analysis. *Mar Ecol Prog Ser* 2013; 490: 199–221. https://doi.org/10.3354/meps10430

[39] Pavlidou A, Velaoras D, Karageorgis AP, et al. Seasonal variations of biochemical and optical properties, physical dynamics and N stable isotopic composition in three northeastern Mediterranean basins (Aegean, Cretan and Ionian Seas). *Deep Sea Research Part II: Topical Studies in Oceanography* 2020; 171: 104704. https://doi.org/10.1016/j.dsr2.2019.104704

[40] Chaikalis S, Parinos C, Möbius J, et al. Optical Properties and Biochemical Indices of Marine Particles in the Open Mediterranean Sea: The R/V Maria S. Merian Cruise, March 2018. *Front Earth Sci*; 9: 614703. https://doi.org/10.3389/feart.2021.614703

[41] Vander Zanden MJ, Rasmussen JB. Variation in $\delta^{15}N$ and $\delta^{13}C$ trophic fractionation: Implications for aquatic food web studies. *Limnol Oceanogr* 2001; 46: 2061–2066. https://doi.org/10.4319/lo.2001.46.8.2061

[42] McCutchan JH, Lewis WM, Kendall C, et al. Variation in trophic shift for stable isotope ratios of carbon, nitrogen, and sulfur. *Oikos* 2003; 102: 378–390. https://doi.org/10.1034/j.1600-0706.2003.12098.x

[43] Pecquerie L, Nisbet RM, Fablet R, et al. The impact of metabolism on stable isotope dynamics: a theoretical framework. *Philosophical Transactions of the Royal Society B: Biological Sciences* 2010; 365: 3455–3468. https://doi.org/10.1098/rstb.2010.0097

[44] Canseco JA, Niklitschek EJ, Harrod C. Variability in $\delta^{13}C$ and $\delta^{15}N$ trophic discrimination factors for teleost fishes: a meta-analysis of temperature and dietary effects. *Rev Fish Biol Fish* 2022; 32: 313–329. https://doi.org/10.1007/s11160-021-09689-1

[45] Arnoldi NS, Litvin SY, Madigan DJ, et al. Multi-taxa marine isoscapes provide insight into large-scale trophic dynamics in the North Pacific. *Prog Oceanogr* 2023; 213: 103005. https://doi.org/10.1016/j.pocean.2023.103005

[46] Berto D, Fanelli E, Vizzini S, et al. ISOMED - A Stable ISOtope database of MEDiterranean marine food web components. *Sci Data* 2025; 12: 1768. https://doi.org/10.1038/s41597-025-05981-y

[47] IsoBank. https://isobank.org/ (accessed 13 November 2025)

[48] IsoArcH. https://isoarch.org/ (accessed 13 November 2025)

[49] Turley CM. The changing Mediterranean Sea – a sensitive ecosystem? *Prog Oceanogr* 1999; 44: 387–400. https://doi.org/10.1016/S0079-6611(99)00033-6

[50] Coll M, Piroddi C, Steenbeek J, et al. The Biodiversity of the Mediterranean Sea: Estimates, Patterns, and Threats. *PLoS One* 2010; 5: e11842. https://doi.org/10.1371/journal.pone.0011842

[51] Lotze HK, Lenihan HS, Bourque BJ, et al. Depletion, Degradation, and Recovery Potential of Estuaries and Coastal Seas. *Science* 2006; 312: 1806–1809. https://doi.org/10.1126/science.1128035

[52] Halpern BS, Walbridge S, Selkoe KA, et al. A Global Map of Human Impact on Marine Ecosystems. *Science* 2008; 319: 948–952. https://doi.org/10.1126/science.1149345

[53] Hilborn R, Amoroso RO, Anderson CM, et al. Effective fisheries management instrumental in improving fish stock status. *Proceedings of the National Academy of Sciences* 2020; 117: 2218–2224. https://doi.org/10.1073/pnas.1909726116

[54] Pisano A, Marullo S, Artale V, et al. New Evidence of Mediterranean Climate Change and Variability from Sea Surface Temperature Observations. *Remote Sens* 2020; 12: 132. https://doi.org/10.3390/rs12010132

[55] Kubin E, Menna M, Mauri E, et al. Heat content and temperature trends in the Mediterranean Sea as derived from Argo float data. *Front Mar Sci* 2023; 10: 1271638. https://doi.org/10.3389/fmars.2023.1271638

[56] Skliris N, Marsh R, Breedon M, et al. Accelerated Warming and Salinification of the Mediterranean Sea: Implications for Dense Water Formation. *J Mar Sci Eng* 2024; 13: 25. https://doi.org/10.3390/jmse13010025

[57] EEA Sea Surface Temperature. https://www.eea.europa.eu/en/analysis/indicators/european-sea-surface-temperature (accessed 13 November 2025)

[58] Vergés A, Steinberg PD, Hay ME, et al. The tropicalization of temperate marine ecosystems: climate-mediated changes in herbivory and community phase shifts. *Proceedings of the Royal Society B: Biological Sciences* 2014; 281: 20140846. https://doi.org/10.1098/rspb.2014.0846

[59] Azzurro E, Sbragaglia V, Cerri J, et al. Climate change, biological invasions, and the shifting distribution of Mediterranean fishes: A large-scale survey based on local ecological knowledge. *Glob Chang Biol* 2019; 25: 2779–2792. https://doi.org/10.1111/gcb.14670

[60] Santana-Garcon J, Bennett S, Marbà N, et al. Tropicalization shifts herbivore pressure from seagrass to rocky reef communities. *Proceedings of the Royal Society B: Biological Sciences* 2023; 290: 20221744. https://doi.org/10.1098/rspb.2022.1744

[61] Raitsos DE, Beaugrand G, Georgopoulos D, et al. Global climate change amplifies the entry of tropical species into the eastern Mediterranean Sea. *Limnol Oceanogr* 2010; 55: 1478–1484. https://doi.org/10.4319/lo.2010.55.4.1478

[62] Fanelli E, Azzurro E, Bariche M, et al. Depicting the novel Eastern Mediterranean food web: a stable isotopes study following Lessepsian fish invasion. *Biol Invasions* 2015; 17: 2163–2178. https://doi.org/10.1007/s10530-015-0868-5

[63] Tiralongo F, Hall-Spencer JM, Giovos I, et al. Editorial: Biological invasions in the Mediterranean Sea. *Front Mar Sci* 2022; 9: 1016168. https://doi.org/10.3389/fmars.2022.1016168

[64] Mackelworth PC, Teff Seker Y, Vega Fernández T, et al. Geopolitics and Marine Conservation: Synergies and Conflicts. *Front Mar Sci* 2019; 6: 759. https://doi.org/10.3389/fmars.2019.00759

[65] Pantoja S, Repeta DJ, Sachs JP, et al. Stable isotope constraints on the nitrogen cycle of the Mediterranean Sea water column. *Deep Sea Research Part I: Oceanographic Research Papers* 2002; 49: 1609–1621. https://doi.org/10.1016/S0967-0637(02)00066-3

[66] Koppelmann R, Weikert H, Lahajnar N. Vertical distribution of mesozooplankton and its $\delta^{15}N$ signature at a deep-sea site in the Levantine Sea (eastern Mediterranean) in April 1999. *J Geophys Res Oceans* 2003; 108: 8118. https://doi.org/10.1029/2002JC001351

[67] Cresson P, Ruitton S, Harmelin-Vivien M. Feeding strategies of co-occurring suspension feeders in an oligotrophic environment. *Food Webs* 2016; 6: 19–28. https://doi.org/10.1016/j.fooweb.2015.12.002

[68] Liénart C, Savoye N, Bozec Y, et al. Dynamics of particulate organic matter composition in coastal systems: A spatio-temporal study at multi-systems scale. *Prog Oceanogr* 2017; 156: 221–239. https://doi.org/10.1016/j.pocean.2017.03.001

[69] Wald T, Fripiat F, Foreman AD, et al. Origins of the Nitrate ^{15}N Depletion in the Mediterranean Sea. *Global Biogeochem Cycles* 2025; 39: e2023GB008035. https://doi.org/10.1029/2023GB008035

[70] Somes CJ, Schmittner A, Muglia J, et al. A Three-Dimensional Model of the Marine Nitrogen Cycle during the Last Glacial Maximum Constrained by Sedimentary Isotopes. *Front Mar Sci* 2017; 4: 108. https://doi.org/10.3389/fmars.2017.00108

[71] Buchanan PJ, Matear RJ, Chase Z, et al. Ocean carbon and nitrogen isotopes in CSIRO Mk3L-COAL version 1.0: a tool for palaeoceanographic research. *Geosci Model Dev* 2019; 12: 1491–1523. https://doi.org/10.5194/gmd-12-1491-2019

[72] Tesi T, Miserocchi S, Goñi MA, et al. Source, transport and fate of terrestrial organic carbon on the western Mediterranean Sea, Gulf of Lions, France. *Mar Chem* 2007; 105: 101–117. https://doi.org/10.1016/j.marchem.2007.01.005

[73] Sanchez-Vidal A, Pasqual C, Kerhervé P, et al. Across margin export of organic matter by cascading events traced by stable isotopes, northwestern Mediterranean Sea. *Limnol Oceanogr* 2009; 54: 1488–1500. https://doi.org/10.4319/lo.2009.54.5.1488

[74] Pedrosa-Pàmies R, Parinos C, Sanchez-Vidal A, et al. Composition and sources of sedimentary organic matter in the deep eastern Mediterranean Sea. *Biogeosciences* 2015; 12: 7379–7402. https://doi.org/10.5194/bg-12-7379-2015

[75] Rumolo P, Cartes JE, Fanelli E, et al. Seasonal variations in the source of sea bottom organic matter off Catalonia coasts (western Mediterranean): links with hydrography and biological response. *J Oceanogr* 2015; 71: 325–343. https://doi.org/10.1007/s10872-015-0291-7

[76] Tesi T, Langone L, Giani M, et al. Source, diagenesis, and fluxes of particulate organic carbon along the western Adriatic Sea (Mediterranean Sea). *Mar Geol* 2013; 337: 156–170. https://doi.org/10.1016/j.margeo.2013.03.001

[77] Ferchiche F, Liénart C, Savoye N, et al. Unlocking the potential of hydrogen isotopes (δ^2H) in tracing riverine particulate organic matter sources and dynamics. *Aquat Sci* 2025; 87: 5. https://doi.org/10.1007/s00027-024-01127-1

[78] Costanzo SD, O'Donohue MJ, Dennison WC, et al. A New Approach for Detecting and Mapping Sewage Impacts. *Mar Pollut Bull* 2001; 42: 149–156. https://doi.org/10.1016/S0025-326X(00)00125-9

[79] Vizzini S, Mazzola A. Stable isotope evidence for the environmental impact of a land-based fish farm in the western Mediterranean. *Mar Pollut Bull* 2004; 49: 61–70. https://doi.org/10.1016/j.marpolbul.2004.01.008

[80] Rumolo P, Barra M, Gherardi S, et al. Stable isotopes and C/N ratios in marine sediments as a tool for discriminating anthropogenic impact. *Journal of Environmental Monitoring* 2011; 13: 3399. https://doi.org/10.1039/c1em10568j

[81] Jona-Lasinio G, Costantini ML, Calizza E, et al. Stable isotope-based statistical tools as ecological indicator of pollution sources in Mediterranean transitional water ecosystems. *Ecol Indic* 2015; 55: 23–31. https://doi.org/10.1016/j.ecolind.2015.03.006

[82] Rossi L, Calizza E, Careddu G, et al. Space-time monitoring of coastal pollution in the Gulf of Gaeta, Italy, using $\delta^{15}N$ values of *Ulva lactuca*, landscape hydromorphology, and Bayesian Kriging modelling. *Mar Pollut Bull* 2018; 126: 479–487. https://doi.org/10.1016/j.marpolbul.2017.11.063

[83] Signa G, Andolina C, Tomasello A, et al. $\delta^{15}N$ in deployed macroalgae as a tool to monitor nutrient input driven by tourism activities in Mediterranean islands. *Mar Pollut Bull* 2020; 159: 111504. https://doi.org/10.1016/j.marpolbul.2020.111504

[84] Thibault M, Duprey N, Gillikin DP, et al. Bivalve $\delta^{15}N$ isoscapes provide a baseline for urban nitrogen footprint at the edge of a World Heritage coral reef. *Mar Pollut Bull* 2020; 152: 110870. https://doi.org/10.1016/j.marpolbul.2019.110870

[85] Chouvelon T, Spitz J, Caurant F, et al. Revisiting the use of $\delta^{15}N$ in meso-scale studies of marine food webs by considering spatio-temporal variations in stable isotopic signatures – The case of an open ecosystem: The Bay of Biscay (North-East Atlantic). *Prog Oceanogr* 2012; 101: 92–105. https://doi.org/10.1016/j.pocean.2012.01.004

[86] Mancinelli G, Vizzini S, Mazzola A, et al. Cross-validation of $\delta^{15}N$ and FishBase estimates of fish trophic position in a Mediterranean lagoon: The importance of the isotopic baseline. *Estuar Coast Shelf Sci* 2013; 135: 77–85. https://doi.org/10.1016/j.ecss.2013.04.004

[87] Reddin CJ, Bothwell JH, O'Connor NE, et al. The effects of spatial scale and isoscape on consumer isotopic niche width. *Funct Ecol* 2018; 32: 904–915. https://doi.org/10.1111/1365-2435.13026

[88] MacKenzie KM, Robertson DR, Adams JN, et al. Structure and nutrient transfer in a tropical pelagic upwelling food web: From isoscapes to the whole ecosystem. *Prog Oceanogr* 2019; 178: 102145. https://doi.org/10.1016/j.pocean.2019.102145

[89] Matich P, Shipley ON, Weideli OC. Quantifying spatial variation in isotopic baselines reveals size-based feeding in a model estuarine predator: implications for trophic studies in dynamic ecotones. *Mar Biol* 2021; 168: 108. https://doi.org/10.1007/s00227-021-03920-0

[90] Merquiol L, Mazzocchi MG, D'Ambra I. The planktonic food web in the Gulf of Naples based on the analysis of carbon and nitrogen stable isotope ratios. *Marine Ecology* 2023; 00: e12762. https://doi.org/10.1111/maec.12762

[91] Trebilco R, Dulvy NK, Anderson SC, et al. The paradox of inverted biomass pyramids in kelp forest fish communities. *Proceedings of the Royal Society B: Biological Sciences* 2016; 283: 20160816. https://doi.org/10.1098/rspb.2016.0816

[92] Travers-Trolet M, Coppin F, Cresson P, et al. Emergence of negative trophic level-size relationships from a size-based, individual-based multispecies fish model. *Ecol Modell* 2019; 410: 108800. https://doi.org/10.1016/j.ecolmodel.2019.108800

[93] Jennings S, Barnes C, Sweeting CJ, et al. Application of nitrogen stable isotope analysis in size-based marine food web and macroecological research. *Rapid Communications in Mass Spectrometry* 2008; 22: 1673–1680. https://doi.org/10.1002/rcm.3497

[94] Navarro J, Coll M, Louzao M, et al. Comparison of ecosystem modelling and isotopic approach as ecological tools to investigate food webs in the NW Mediterranean Sea. *J Exp Mar Biol Ecol* 2011; 401: 97–104. https://doi.org/10.1016/j.jembe.2011.02.040

[95] Pacella SR, Lebreton B, Richard P, et al. Incorporation of diet information derived from Bayesian stable isotope mixing models into mass-balanced marine ecosystem models: A case study from the Marennes-Oléron Estuary, France. *Ecol Modell* 2013; 267: 127–137. https://doi.org/10.1016/j.ecolmodel.2013.07.018

[96] Pethybridge HR, Choy CA, Polovina JJ, et al. Improving Marine Ecosystem Models with Biochemical Tracers. *Ann Rev Mar Sci* 2018; 10: 199–228. https://doi.org/10.1146/annurev-marine-121916-063256

[97] McCormack SA, Trebilco R, Melbourne-Thomas J, et al. Using stable isotope data to advance marine food web modelling. *Rev Fish Biol Fish* 2019; 29: 277–296. https://doi.org/10.1007/s11160-019-09552-4

[98] Darnaude AM, Salen-Picard C, Polunin NVC, et al. Trophodynamic Linkage between River Runoff and Coastal Fishery Yield Elucidated by Stable Isotope Data in the Gulf of Lions (NW Mediterranean). *Oecologia* 2004; 138: 325–332. https://doi.org/10.1007/s00442-003-1457-3

[99] Darnaude AM. Fish ecology and terrestrial carbon use in coastal areas: implications for marine fish production. *Journal of Animal Ecology* 2005; 74: 864–876. https://doi.org/10.1111/j.1365-2656.2005.00978.x

[100] Harmelin-Vivien M, Loizeau V, Mellon C, et al. Comparison of C and N stable isotope ratios between surface particulate organic matter and microphytoplankton in the Gulf of Lions (NW Mediterranean). *Cont Shelf Res* 2008; 28: 1911–1919. https://doi.org/10.1016/j.csr.2008.03.002

[101] Fanelli E, Cartes JE, Rumolo P, et al. Food-web structure and trophodynamics of mesopelagic–suprabenthic bathyal macrofauna of the Algerian Basin based on stable isotopes of carbon and nitrogen. *Deep Sea Research Part I: Oceanographic Research Papers* 2009; 56: 1504–1520. https://doi.org/10.1016/j.dsr.2009.04.004

[102] Fanelli E, Cartes JE, Papiol V. Food web structure of deep-sea macrozooplankton and micronekton off the Catalan slope: Insight from stable isotopes. *Journal of Marine Systems* 2011; 87: 79–89. https://doi.org/10.1016/j.jmarsys.2011.03.003

[103] Papiol V, Cartes JE, Fanelli E, et al. Food web structure and seasonality of slope megafauna in the NW Mediterranean elucidated by stable isotopes: Relationship with available food sources. *J Sea Res* 2013; 77: 53–69. https://doi.org/10.1016/j.seares.2012.10.002

[104] Valls M, Sweeting CJ, Olivar MP, et al. Structure and dynamics of food webs in the water column on shelf and slope grounds of the western Mediterranean. *Journal of Marine Systems* 2014; 138: 171–181. https://doi.org/10.1016/j.jmarsys.2014.04.002

[105] Coppari M, Ferrier-Pagès C, Castellano M, et al. Seasonal variation of the stable C and N isotopic composition of the mesophotic black coral *Antipathella subpinnata* (Ellis & Solander, 1786). *Estuar Coast Shelf Sci* 2020; 233: 106520. https://doi.org/10.1016/j.ecss.2019.106520

[106] Masiá P, Sozio J, Da Ros Z, et al. At the base of deep-sea food webs: Assemblage and trophic structure of suprabenthos and zooplankton in submarine canyons. *Prog Oceanogr* 2024; 228: 103318. https://doi.org/10.1016/j.pocean.2024.103318

[107] Cobain MRD, Magozzi S, Vane K, et al. Spatially explicit estimates of benthic-pelagic coupling strength using a dual isoscape approach. In prep.

[108] Wunder MB. Using Isoscapes to Model Probability Surfaces for Determining Geographic Origins. In: *Isoscapes: Understanding movement, pattern, and process on Earth through isotope mapping*. Springer Dordrecht, 2010, pp. 251–270. https://doi.org/10.1007/978-90-481-3354-3_12

[109] Ma C, Vander Zanden HB, Wunder MB, et al. assignR: An r package for isotope-based geographic assignment. *Methods Ecol Evol* 2020; 11: 996–1001. https://doi.org/10.1111/2041-210X.13426

[110] Carpenter-Kling T, Pistorius P, Connan M, et al. Sensitivity of $\delta^{13}C$ values of seabird tissues to combined spatial, temporal and ecological drivers: A simulation approach. *J Exp Mar Biol Ecol* 2019; 512: 12–21. https://doi.org/10.1016/j.jembe.2018.12.007

[111] Jaeger A, Lecomte VJ, Weimerskirch H, et al. Seabird satellite tracking validates the use of latitudinal isoscapes to depict predators' foraging areas in the Southern Ocean. *Rapid Communications in Mass Spectrometry* 2010; 24: 3456–3460. https://doi.org/10.1002/rcm.4792

[112] St John Glew K, Wanless S, Harris MP, et al. Moult location and diet of auks in the North Sea inferred from coupled light-based and isotope-based geolocation. *Mar Ecol Prog Ser* 2018; 599: 239–251. https://doi.org/10.3354/meps12624

[113] Arcioni M, D'Ambra I, Vizzini S, et al. Trophic ecology of the deep-sea skate *Dipturus oxyrinchus* (Linnaeus, 1758) in the bathyal food web of the central Mediterranean Sea. *Deep Sea Research Part I: Oceanographic Research Papers* 2025; 225: 104602. https://doi.org/10.1016/j.dsr.2025.104602

[114] McCauley DJ, Young HS, Dunbar RB, et al. Assessing the effects of large mobile predators on ecosystem connectivity. *Ecological Applications* 2012; 22: 1711–1717. https://doi.org/10.1890/11-1653.1
[115] Shipley ON, Matich P, Hussey NE, et al. Energetic connectivity of diverse elasmobranch populations – implications for ecological resilience. *Proceedings of the Royal Society B: Biological Sciences* 2023; 290: 20230262. https://doi.org/10.1098/rspb.2023.0262
[116] MacKenzie KM, Palmer MR, Moore A, et al. Locations of marine animals revealed by carbon isotopes. *Sci Rep* 2011; 1: 21. https://doi.org/10.1038/srep00021
[117] Hungate BA, Kearns DN, Ogle K, et al. Hydrogen Isotopes as a Sentinel of Biological Invasion by the Japanese Beetle, *Popillia japonica* (Newman). *PLoS One* 2016; 11: e0149599. https://doi.org/10.1371/journal.pone.0149599
[118] McCue MD, Javal M, Clusella-Trullas S, et al. Using stable isotope analysis to answer fundamental questions in invasion ecology: Progress and prospects. *Methods Ecol Evol* 2020; 11: 196–214. https://doi.org/10.1111/2041-210X.13327
[119] Bernardi G, Azzurro E, Bariche M, et al. Invasion genomics of lionfish in the Mediterranean Sea. *Ecol Evol* 2024; 14: e11087. https://doi.org/10.1002/ece3.11087
[120] Fanelli E, Menicucci S, Malavolti S, et al. Spatial changes in community composition and food web structure of mesozooplankton across the Adriatic basin (Mediterranean Sea). *Biogeosciences* 2022; 19: 1833–1851. https://doi.org/10.5194/bg-19-1833-2022
[121] Breton E, Savoye N, Rimmelin-Maury P, et al. Data quality control considerations in multivariate environmental monitoring: experience of the French coastal network SOMLIT. *Front Mar Sci* 2023; 10: 1135446. https://doi.org/10.3389/fmars.2023.1135446
[122] Liénart C, Fournioux A, Garbaras A, et al. Bivalve monitoring over French coasts: multi-decadal records of carbon and nitrogen elemental and isotopic ratios as ecological indicators of global change. *Earth Syst Sci Data* 2025; 17: 799–815. https://doi.org/10.5194/essd-17-799-2025
[123] Protopapa M, Herrera Rivero I, Wilhelm H, et al. Advancing Food Web Monitoring: Integrating Biomarkers for Zooplankton Assessment. 2025.
[124] McCook LJ, Almany GR, Berumen ML, et al. Management under uncertainty: guide-lines for incorporating connectivity into the protection of coral reefs. *Coral Reefs* 2009; 28: 353–366. https://doi.org/10.1007/s00338-008-0463-7
[125] Vizzini S, Mazzola A. Stable isotopes and trophic positions of littoral fishes from a Mediterranean marine protected area. *Environ Biol Fishes* 2009; 84: 13–25. https://doi.org/10.1007/s10641-008-9381-3
[126] Foley MM, Halpern BS, Micheli F, et al. Guiding ecological principles for marine spatial planning. *Mar Policy* 2010; 34: 955–966. https://doi.org/10.1016/j.marpol.2010.02.001
[127] Jennings S, Greenstreet S, Hill L, et al. Long-term trends in the trophic structure of the North Sea fish community: evidence from stable-isotope analysis, size-spectra and community metrics. *Mar Biol* 2002; 141: 1085–1097. https://doi.org/10.1007/s00227-002-0905-7
[128] Pinnegar JK, Polunin NVC, Badalamenti F. Long-term changes in the trophic level of western Mediterranean fishery and aquaculture landings. *Canadian Journal of Fisheries and Aquatic Sciences* 2003; 60: 222–235. https://doi.org/10.1139/f03-016
[129] Rumolo P, Fanelli E, Barra M, et al. Trophic relationships between anchovy (*Engraulis encrasicolus*) and zooplankton in the Strait of Sicily (Central Mediterranean sea): a stable isotope approach. *Hydrobiologia* 2018; 821: 41–56. https://doi.org/10.1007/s10750-017-3334-9
[130] Agnetta D, Badalamenti F, Sweeting CJ, et al. Erosion of fish trophic position: an indirect effect of fishing on food webs elucidated by stable isotopes. *Philosophical Transactions of the Royal Society B: Biological Sciences* 2024; 379: 20230167. https://doi.org/10.1098/rstb.2023.0167

[131] Di Lorenzo M, Vizzini S, Signa G, et al. Ontogenetic trophic segregation between two threatened smooth-hound sharks in the Central Mediterranean Sea. *Sci Rep* 2020; 10: 11011. https://doi.org/10.1038/s41598-020-67858-x

[132] Smith KJ, Trueman CN, France CAM, et al. Stable Isotope Analysis of Specimens of Opportunity Reveals Ocean-Scale Site Fidelity in an Elusive Whale Species. *Frontiers in Conservation Science* 2021; 2: 653766. https://doi.org/10.3389/fcosc.2021.653766

[133] Salgado-Hernanz PM, Racault M-F, Font-Muñoz JS, et al. Trends in phytoplankton phenology in the Mediterranean Sea based on ocean-colour remote sensing. *Remote Sens Environ* 2019; 221: 50–64. https://doi.org/10.1016/j.rse.2018.10.036

[134] Reale M, Cossarini G, Lazzari P, et al. Acidification, deoxygenation, and nutrient and biomass declines in a warming Mediterranean Sea. *Biogeosciences* 2022; 19: 4035–4065. https://doi.org/10.5194/bg-19-4035-2022

[135] Salgado-Hernanz PM, Regaudie-de-Gioux A, Antoine D, et al. Pelagic primary production in the coastal Mediterranean Sea: variability, trends, and contribution to basin-scale budgets. *Biogeosciences* 2022; 19: 47–69. https://doi.org/10.5194/bg-19-47-2022

[136] Álvarez M, Catalá TS, Civitarese G, et al. Mediterranean Sea general biogeochemistry. In: *Oceanography of the Mediterranean Sea*. Elsevier, 2023, pp. 387–451. https://doi.org/10.1016/B978-0-12-823692-5.00004-2

[137] Rau GH, Takahashi T, Marais DJ Des. Latitudinal variations in plankton $\delta^{13}C$: implications for CO2 and productivity in past oceans. *Nature* 1989; 341: 516–518. https://doi.org/10.1038/341516a0

[138] Rau GH, Riebesell U, Wolf-Gladrow D. A model of photosynthetic ^{13}C fractionation by marine phytoplankton based on diffusive molecular CO_2 uptake. *Mar Ecol Prog Ser* 1996; 133: 275–285. https://doi.org/10.3354/meps133275

[139] Rau GH, Riebesell U, Wolf-Gladrow D. CO_{2aq}-dependent photosynthetic ^{13}C fractionation in the ocean: A model versus measurements. *Global Biogeochem Cycles* 1997; 11: 267–278. https://doi.org/10.1029/97GB00328

[140] Laws EA, Popp BN, Bidigare RR, et al. Dependence of phytoplankton carbon isotopic composition on growth rate and [CO_{2aq}]: Theoretical considerations and experimental results. *Geochim Cosmochim Acta* 1995; 59: 1131–1138. https://doi.org/10.1016/0016-7037(95)00030-4

[141] Laws EA, Bidigare RR, Popp BN. Effect of growth rate and CO_2 concentration on carbon isotopic fractionation by the marine diatom *Phaeodactylum tricornutum*. *Limnol Oceanogr* 1997; 42: 1552–1560. https://doi.org/10.4319/lo.1997.42.7.1552

[142] Ryabenko E. Stable Isotope Methods for the Study of the Nitrogen Cycle. In: *Topics in Oceanography*. InTech, 2013. http://dx.doi.org/10.5772/56105

[143] Mara P, Mihalopoulos N, Gogou A, et al. Isotopic composition of nitrate in wet and dry atmospheric deposition on Crete in the eastern Mediterranean Sea. *Global Biogeochem Cycles* 2009; 23: GB4002. https://doi.org/10.1029/2008GB003395

[144] Emeis K-C, Mara P, Schlarbaum T, et al. External N inputs and internal N cycling traced by isotope ratios of nitrate, dissolved reduced nitrogen, and particulate nitrogen in the eastern Mediterranean Sea. *J Geophys Res Biogeosci* 2010; 115: G04041. https://doi.org/10.1029/2009JG001214

[145] Krom MD, Emeis K-C, Van Cappellen P. Why is the Eastern Mediterranean phosphorus limited? *Prog Oceanogr* 2010; 85: 236–244. https://doi.org/10.1016/j.pocean.2010.03.003

[146] Tecchio S, van Oevelen D, Soetaert K, et al. Trophic Dynamics of Deep-Sea Megabenthos Are Mediated by Surface Productivity. *PLoS One* 2013; 8: 1–8. https://doi.org/10.1371/journal.pone.0063796

[147] Struck U, Emeis K-C, Voß M, et al. Biological productivity during sapropel S5 formation in the Eastern Mediterranean Sea: evidence from stable isotopes of nitrogen and carbon. *Geochim Cosmochim Acta* 2001; 65: 3249–3266. https://doi.org/10.1016/S0016-7037(01)00668-8
[148] Madurell T, Fanelli E, Cartes JE. Isotopic composition of carbon and nitrogen of suprabenthic fauna in the NW Balearic Islands (western Mediterranean). *Journal of Marine Systems* 2008; 71: 336–345. https://doi.org/10.1016/j.jmarsys.2007.03.006
[149] Barnes C, Jennings S, Barry JT. Environmental correlates of large-scale spatial variation in the $\delta^{13}C$ of marine animals. *Estuar Coast Shelf Sci* 2009; 81: 368–374. https://doi.org/10.1016/j.ecss.2008.11.011
[150] Copernicus Marine Service (CMEMS). https://data.marine.copernicus.eu/products (accessed 13 November 2025)
[151] Escudier R, Clementi E, Cipollone A, et al. A High Resolution Reanalysis for the Mediterranean Sea. *Front Earth Sci* 2021; 9: 702285. https://doi.org/10.3389/feart.2021.702285
[152] Cossarini G, Feudale L, Teruzzi A, et al. High-Resolution Reanalysis of the Mediterranean Sea Biogeochemistry (1999–2019). *Front Mar Sci* 2021; 8: 741486. https://doi.org/10.3389/fmars.2021.741486
[153] Hecht A, Pinardi N, Robinson AR. Currents, Water Masses, Eddies and Jets in the Mediterranean Levantine Basin. *J Phys Oceanogr* 1988; 18: 1320–1353. https://doi.org/10.1175/1520-0485(1988)018<1320:CWMEAJ>2.0.CO;2
[154] Benincasa R, Liguori G, Pinardi N, et al. Internal and forced ocean variability in the Mediterranean Sea. *Ocean Science* 2024; 20: 1003–1012. https://doi.org/10.5194/os-20-1003-2024
[155] van Etten J. R Package gdistance: Distances and Routes on Geographical Grids. *J Stat Softw* 2017; 76: 1–21. https://doi.org/10.18637/jss.v076.i13
[156] Zuur AF, Ieno EN, Saveliev AA. *Beginner's guide to spatial, temporal, and spatial-temporal ecological data analysis with R-INLA*. Highland Statistics Ltd, 2017.
[157] R-INLA. http://www.r-inla.org (accessed 13 November 2025)
[158] Rue H, Martino S, Chopin N. Approximate Bayesian inference for latent Gaussian models by using integrated nested Laplace approximations. *J R Stat Soc Series B Stat Methodol* 2009; 71: 319–392. https://doi.org/10.1111/j.1467-9868.2008.00700.x
[159] Pierre C. The oxygen and carbon isotope distribution in the Mediterranean water masses. *Mar Geol* 1999; 153: 41–55. https://doi.org/10.1016/S0025-3227(98)00090-5
[160] Sisma-Ventura G, Yam R, Kress N, et al. Water column distribution of stable isotopes and carbonate properties in the South-eastern Levantine basin (Eastern Mediterranean): Vertical and temporal change. *Journal of Marine Systems* 2016; 158: 13–25. https://doi.org/10.1016/j.jmarsys.2016.01.012
[161] Cartes JE, Fanelli E, Kapiris K, et al. Spatial variability in the trophic ecology and biology of the deep-sea shrimp *Aristaeomorpha foliacea* in the Mediterranean Sea. *Deep Sea Research Part I: Oceanographic Research Papers* 2014; 87: 1–13. https://doi.org/10.1016/j.dsr.2014.01.006
[162] David Wells RJ, Rooker JR, Addis P, et al. Regional patterns of $\delta^{13}C$ and $\delta^{15}N$ for European common cuttlefish (*Sepia officinalis*) throughout the Northeast Atlantic Ocean and Mediterranean Sea. *R Soc Open Sci* 2021; 8: 210345. https://doi.org/10.1098/rsos.210345
[163] Andrews AJ, Pampoulie C, Di Natale A, et al. Exploitation shifted trophic ecology and habitat preferences of Mediterranean and Black Sea bluefin tuna over centuries. *Fish and Fisheries* 2023; 24: 1067–1083. https://doi.org/10.1111/faf.12785
[164] Cardona L, Clusa M, Eder E, et al. Distribution patterns and foraging ground productivity determine clutch size in Mediterranean loggerhead turtles. *Mar Ecol Prog Ser* 2014; 497: 229–241. https://doi.org/10.3354/meps10595

[165] Jennings S, Reñones O, Morales-Nin B, et al. Spatial variation in the ^{15}N and ^{13}C stable isotope composition of plants, invertebrates and fishes on Mediterranean reefs: implications for the study of trophic pathways. *Mar Ecol Prog Ser* 1997; 146: 109–116. https://doi.org/10.3354/meps146109

[166] Rumolo P, Bonanno A, Barra M, et al. Spatial variations in feeding habits and trophic levels of two small pelagic fish species in the central Mediterranean Sea. *Mar Environ Res* 2016; 115: 65–77. https://doi.org/10.1016/j.marenvres.2016.02.004

[167] Ibello V, Cantoni C, Cozzi S, et al. First basin-wide experimental results on N_2 fixation in the open Mediterranean Sea. *Geophys Res Lett* 2010; 37: L03608. https://doi.org/10.1029/2009GL041635

[168] Benavides M, Bonnet S, Hernández N, et al. Basin-wide N_2 fixation in the deep waters of the Mediterranean Sea. *Global Biogeochem Cycles* 2016; 30: 952–961. https://doi.org/10.1002/2015GB005326

[169] Bonnet S, Grosso O, Moutin T. Planktonic dinitrogen fixation along a longitudinal gradient across the Mediterranean Sea during the stratified period (BOUM cruise). *Biogeosciences* 2011; 8: 2257–2267. https://doi.org/10.5194/bg-8-2257-2011

[170] Rahav E, Herut B, Levi A, et al. Springtime contribution of dinitrogen fixation to primary production across the Mediterranean Sea. *Ocean Sci* 2013; 9: 489–498. https://doi.org/10.5194/os-9-489-2013

[171] Ridame C, Dinasquet J, Hallstrøm S, et al. N_2 fixation in the Mediterranean Sea related to the composition of the diazotrophic community and impact of dust under present and future environmental conditions. *Biogeosciences* 2022; 19: 415–435. https://doi.org/10.5194/bg-19-415-2022

[172] Millot C, Taupier-Letage I. Circulation in the Mediterranean Sea. In: *The Mediterranean Sea*. Springer, Berlin, Heidelberg, 2005, pp. 29–66. https://doi.org/10.1007/b107143

[173] Cresson P, Ruitton S, Fontaine M-F, et al. Spatio-temporal variation of suspended and sedimentary organic matter quality in the Bay of Marseilles (NW Mediterranean) assessed by biochemical and isotopic analyses. *Mar Pollut Bull* 2012; 64: 1112–1121. https://doi.org/10.1016/j.marpolbul.2012.04.003

[174] Miller R, Page H, Brzezinski M. $\delta^{13}C$ and $\delta^{15}N$ of particulate organic matter in the Santa Barbara Channel: drivers and implications for trophic inference. *Mar Ecol Prog Ser* 2013; 474: 53–66. https://doi.org/10.3354/meps10098

[175] Chen C-T, Carlotti F, Harmelin-Vivien M, et al. Isotopic and biochemical trophic markers reveal the complexity of interactions at the base of pelagic food webs (Mediterranean sea). *Mar Environ Res* 2023; 190: 106123. https://doi.org/10.1016/j.marenvres.2023.106123

[176] DeNiro MJ, Epstein S. Influence of diet on the distribution of carbon isotopes in animals. *Geochim Cosmochim Acta* 1978; 42: 495–506. https://doi.org/10.1016/0016-7037(78)90199-0

[177] DeNiro MJ, Epstein S. Influence of diet on the distribution of nitrogen isotopes in animals. *Geochim Cosmochim Acta* 1981; 45: 341–351. https://doi.org/10.1016/0016-7037(81)90244-1

[178] Post DM. USING STABLE ISOTOPES TO ESTIMATE TROPHIC POSITION: MODELS, METHODS, AND ASSUMPTIONS. *Ecology* 2002; 83: 703–718. https://doi.org/10.1890/0012-9658(2002)083[0703:USITET]2.0.CO;2

[179] Savoye N, Aminot A, Tréguer P, et al. Dynamics of particulate organic matter d15N and d13C during spring phytoplankton blooms in a macrotidal ecosystem (Bay of Seine, France). *Mar Ecol Prog Ser* 2003; 255: 27–41. https://doi.org/10.3354/meps255027

[180] Valls M, Olivar MP, Fernández de Puelles ML, et al. Trophic structure of mesopelagic fishes in the western Mediterranean based on stable isotopes of carbon and nitrogen. *Journal of Marine Systems* 2014; 138: 160–170. https://doi.org/10.1016/j.jmarsys.2014.04.007

[181] Pasqual C, Calafat A, Lopez-Fernandez P, et al. Organic carbon inputs to the sea bottom of the Mallorca continental slope. *Journal of Marine Systems* 2015; 148: 142–151. https://doi.org/10.1016/j.jmarsys.2015.02.006

[182] Skinner C, Cobain MRD, Zhu Y, et al. Progress and Direction in the Use of Stable Isotopes to Understand Complex Coral Reef Ecosystems: A Review. In: *Oceanography and Marine Biology: An Annual Review,* CRC Press, 2022, pp. 373–432. https://doi.org/10.1201/9781003288602-8

[183] Richardson AJ, Walne AW, John AWG, et al. Using continuous plankton recorder data. *Prog Oceanogr* 2006; 68: 27–74. https://doi.org/10.1016/j.pocean.2005.09.011

[184] Silva MA, Fonseca CT, Olivar MP, et al. MesopTroph, a database of trophic parameters to study interactions in mesopelagic food webs. *Sci Data* 2022; 9: 716. https://doi.org/10.1038/s41597-022-01831-3

[185] Perga ME, Bouletreau S, Cucherousset J, et al. A global estimator of C and N isotope baselines for fresh waters. *Methods in Ecology and Evolution* 2026, 17: 992–1006. https://doi.org/10.1111/2041-210x.70225

[186] Tesán-Onrubia JA, Tedetti M, Carlotti F, et al. Spatial variations of biochemical content and stable isotope ratios of size-fractionated plankton in the Mediterranean Sea (MERITE-HIPPOCAMPE campaign). *Mar Pollut Bull* 2023; 189: 114787. https://doi.org/10.1016/j.marpolbul.2023.114787

[187] GEOTRACES. https://www.geotraces.org/ (accessed 13 November 2025)

[188] Spedicato MT, Massutí E, Mérigot B, et al. The MEDITS trawl survey specifications in an ecosystem approach to fishery management. *Sci Mar* 2019; 83: 9–20. DOI: 10.3989/scimar.04915.11X

[189] Giannoulaki M, Zwolinski J, Gucu AC, et al. The "MEDiterranean International Acoustic Survey": An introduction. *Mediterr Mar Sci* 2021; 22: 747–750. https://doi.org/10.12681/mms.29068

[190] Ifremer. Oceanographic campaign – PELMED (PELagic MEDiterranée), FR-DCSMM-PDS-PELMED. Digital Profile and Metadata. Laboratoire Halieutique Méditerranée, Ifremer, Sète. 2022. https://sextant.ifremer.fr/geonetwork/srv/api/records/81834290-2946-4fb7-93b1-7d1655ef80f3 (accessed 13 November 2025)

[191] de Boois. *Moving towards integrated ecosystem monitoring. ICES Cooperative Research Reports* 2019. https://doi.org/10.17895/ices.pub.4703

[192] EU. *Directive 2008/56/EC of the European Parliament and of the Council establishing a framework for community action in the field of marine environmental policy (Marine Strategy Framework Directive). Official Journal of the European Union L164, 9–40*. 2008.

[193] Rumolo P, Barra M, Bonanno A, et al. Spatiotemporal variability in the feeding habits of anchovy and sardine: a comparison of upwelling and river-runoff driven ecosystems. *Front Mar Sci* 2025; 12: 1602042. https://doi.org/10.3389/fmars.2025.160204

[194] Ortiz JJ, Preciado I, Hidalgo M, et al. Estimating spatial variability of baseline isoscapes from fish isotopic signatures at the community level. *Prog Oceanogr* 2024; 221: 103205. https://doi.org/10.1016/j.pocean.2024.103205

[195] Cartes JE, Papiol V, Santos-Echeandía J, et al. Analysis of communities, with an historical reconstruction from a deep submarine seamount in an oligotrophic area (Valencia Seamount, Balearic Basin, Western Mediterranean). *Deep Sea Research Part I: Oceanographic Research Papers* 2024; 209: 104325. https://doi.org/10.1016/j.dsr.2024.104325

[196] Bury S, Peters K, Sabadel A, et al. Southern Ocean humpback whale trophic ecology. I. Combining multiple stable isotope methods elucidates diet, trophic position and foraging areas. *Mar Ecol Prog Ser* 2024; 734: 123–155. https://doi.org/10.3354/meps14532

[197] Kerr MR, Currie N, Kosnik MA, et al. Regional databases demonstrate macroecological patterns less clearly than systematically collected field data. *Ecography* 2025; 2025: e07355. https://doi.org/10.1111/ecog.07355

[198] Courtiol A, Rousset F. Modelling isoscapes using mixed models. *bioRxiv* 2017; 207662. https://doi.org/10.1101/207662

Magozzi et al. – figure captions

Figure 1. Conceptual overview of the main data inputs for INLA models: environmental data layers (A), spatial distribution of isotope observations (B), and non-spatial sources of isotope variability within the dataset (C). Panel A shows three example environmental layers - sea surface temperature (SST [°C]), chlorophyll *a* concentration (Chl [mg m^{-3}]), and nitrate concentration (NO_3^- [mmol m^{-3}]) - illustrating basin-scale gradients in temperature, productivity, and nutrient availability across the Mediterranean Sea. Covariates are shown as mean-centered annual averages of multi-year climatologies. Additional environmental variables and principal component analyses are presented in Fig. S.5 and S.6. Panel B shows sampling locations of isotope observations, with circle size proportional to the number of observations per location. International Hydrographic Organization (IHO) sea area boundaries are indicated (Gib/Alb = Strait of Gibraltar/Alboran Sea, Bal = Balearic Sea, Lig = Ligurian Sea, Tyrr = Tyrrhenian Sea, NWMed = North-Western Mediterranean Sea, Adr = Adriatic Sea, Ion = Ionian Sea, Aeg = Aegean Sea, EMed = Eastern Mediterranean See; see Fig. A.1). Observations are pooled across $\delta^{15}N$ and $\delta^{13}C$; isotope-specific distributions are shown in Fig. S.2A, B. Panel C shows the proportional representation of category, depth zone, and season across IHO sea areas, based on pooled observations. Isotope-specific proportions are provided in Fig. S.2C, D (category), S.3 (depth), and S.4 (season). Additional sources of isotopic variability include year, taxonomy, biological and ecological traits, trophic structure, and sampling and analytical methods.

Figure 2. Sample semivariograms of $\delta^{15}N$ (A) and (B) $\delta^{13}C$ reference data computed using least-cost geographic distance across the Mediterranean Sea. Panels C and D show the number of sample pairs per distance bin; support declines substantially beyond ca. 2500 km.

Figure 3. Posterior probability distributions of the spatial field range parameter for $\delta^{15}N$ (A) and $\delta^{13}C$ (B) models. All models include the spatial field and category as random effects. Models shown are: (i) null spatial models without covariates (M0.SF), ii) models with covariates as linear fixed effects (M1lin.SF), and iii) models with covariates as smooth terms (M1sm.SF). Thicker lines indicate the best-performing models based on WAIC (M1sm.SF for $\delta^{15}N$ and M0.SF for $\delta^{13}C$).

Figure 4. Marginal posterior distributions of the category random effect for $\delta^{15}N$ (A) and $\delta^{13}C$ (B) models. Each distribution ($\pi \mid D$) represents the probability density of the deviation of a given category from the overall mean isotope value, conditional on the data. Distributions are derived from the best-performing models (M1sm.SF for $\delta^{15}N$ and M0.SF for $\delta^{13}C$).

Figure 5. Predicted isoscape surfaces for $\delta^{15}N$ (A, C) and $\delta^{13}C$ (B, D) across the Mediterranean Sea. Panels show posterior means (A, B) and posterior variances (C, D) predicted by the best-performing models (M1sm.SF for $\delta^{15}N$ and M0.SF for $\delta^{13}C$). Variances are displayed on a $\log_{10}$ color scale for visualization. Points indicate sampling locations. Predictions represent geographic baseline isoscapes derived from six sample categories representing low-trophic-level food web compartments primarily supported by epipelagic production. Category was included as a non-spatial random effect to account for systematic differences among groups.

Declaration of interests

☒ The authors declare that they have no known competing financial interests or personal relationships that could have appeared to influence the work reported in this paper.

☐ The authors declare the following financial interests/personal relationships which may be considered as potential competing interests: